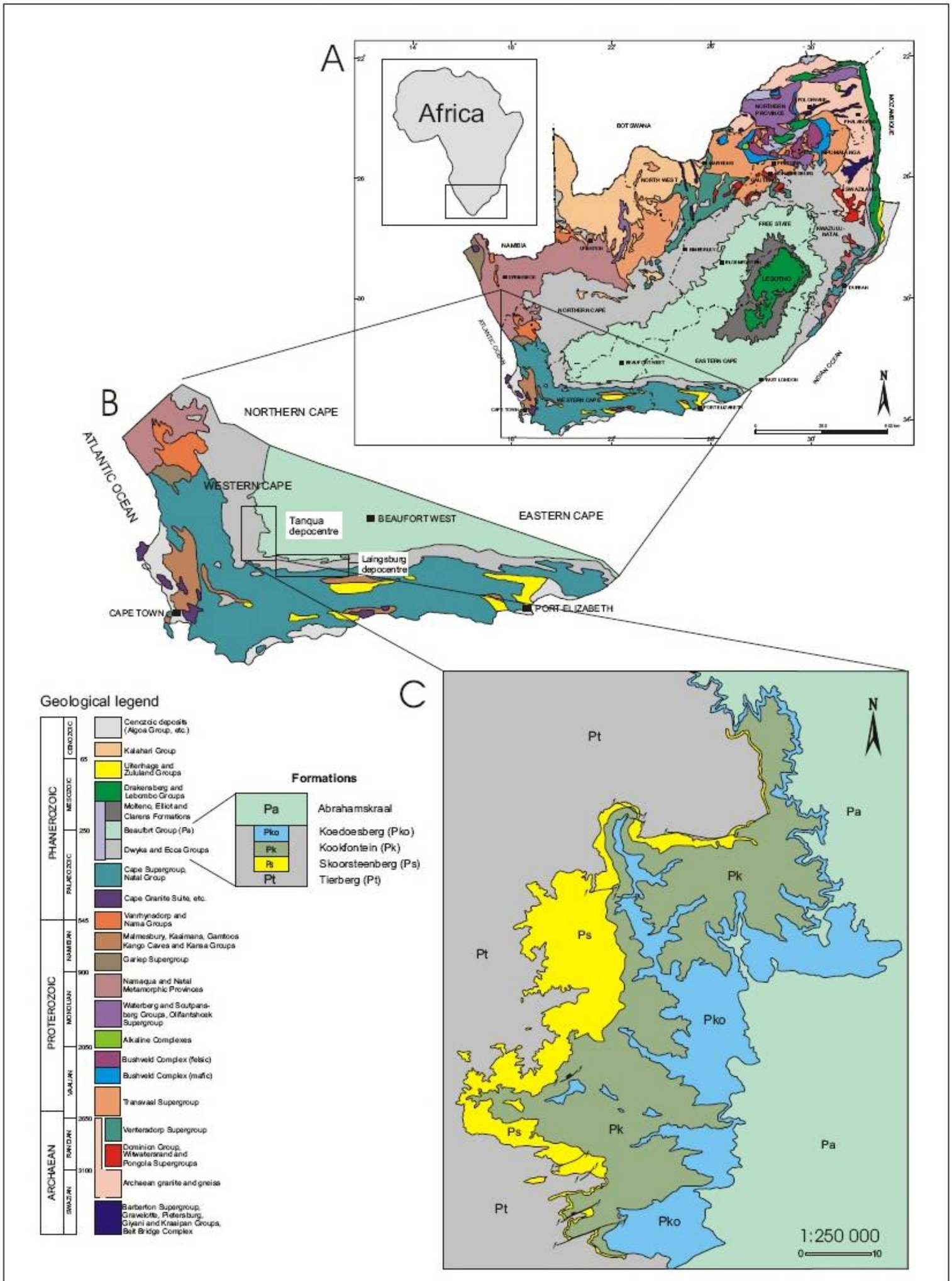

Figure 1: Simplified geological map of South Africa (A), the Western Cape (B) and the Tanqua sub-basin (C) (Geological map of South Africa, Council for Geoscience, 2000; Tanqua sub-basin map after Van der Merwe, 2003).

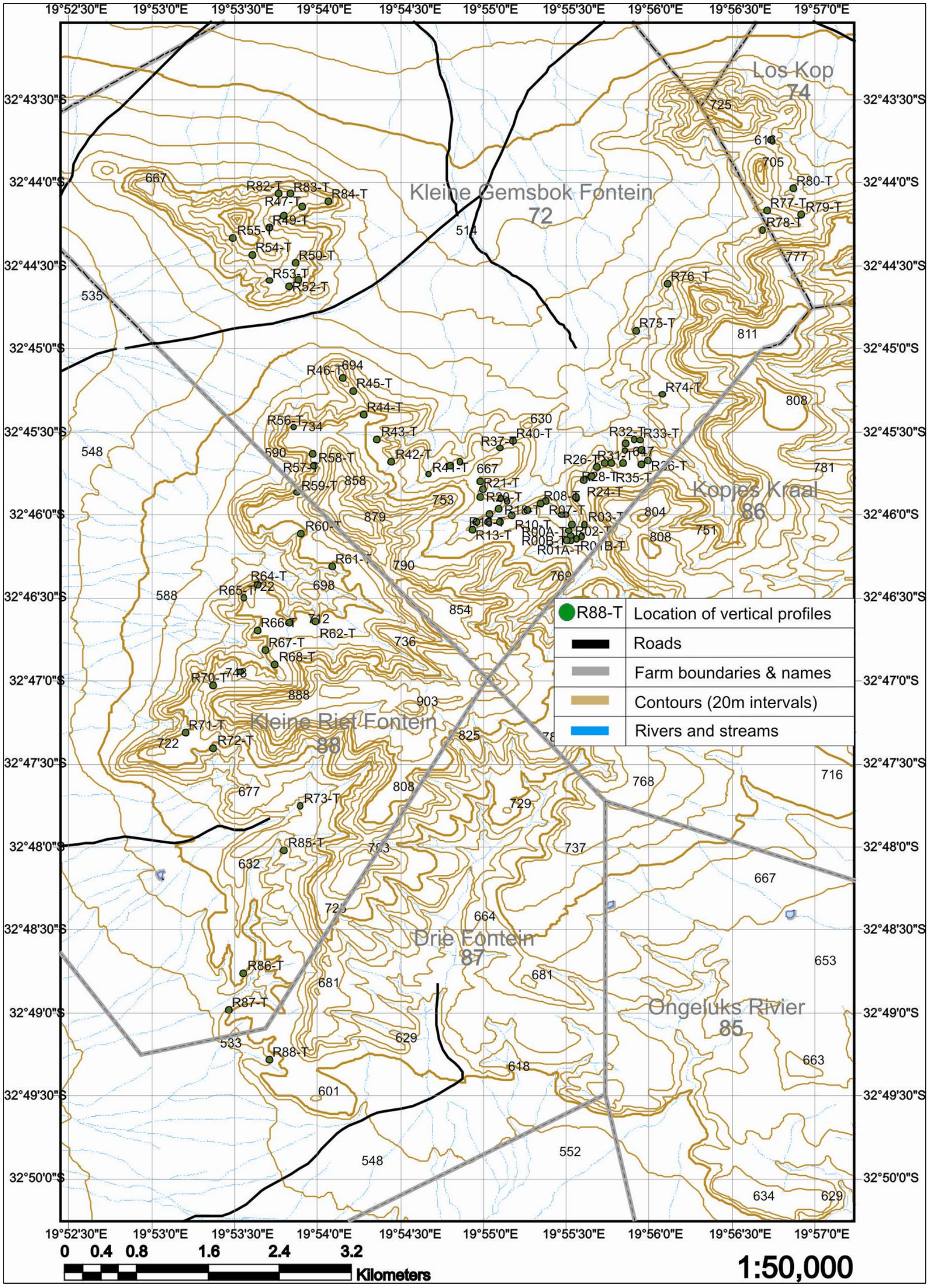

Figure 7: 1:50 000 ArcView map shows the localities of the 91 vertical profiles in the study area (green dots), farm names and boundaries (grey) and 20 m interval contours (brown).

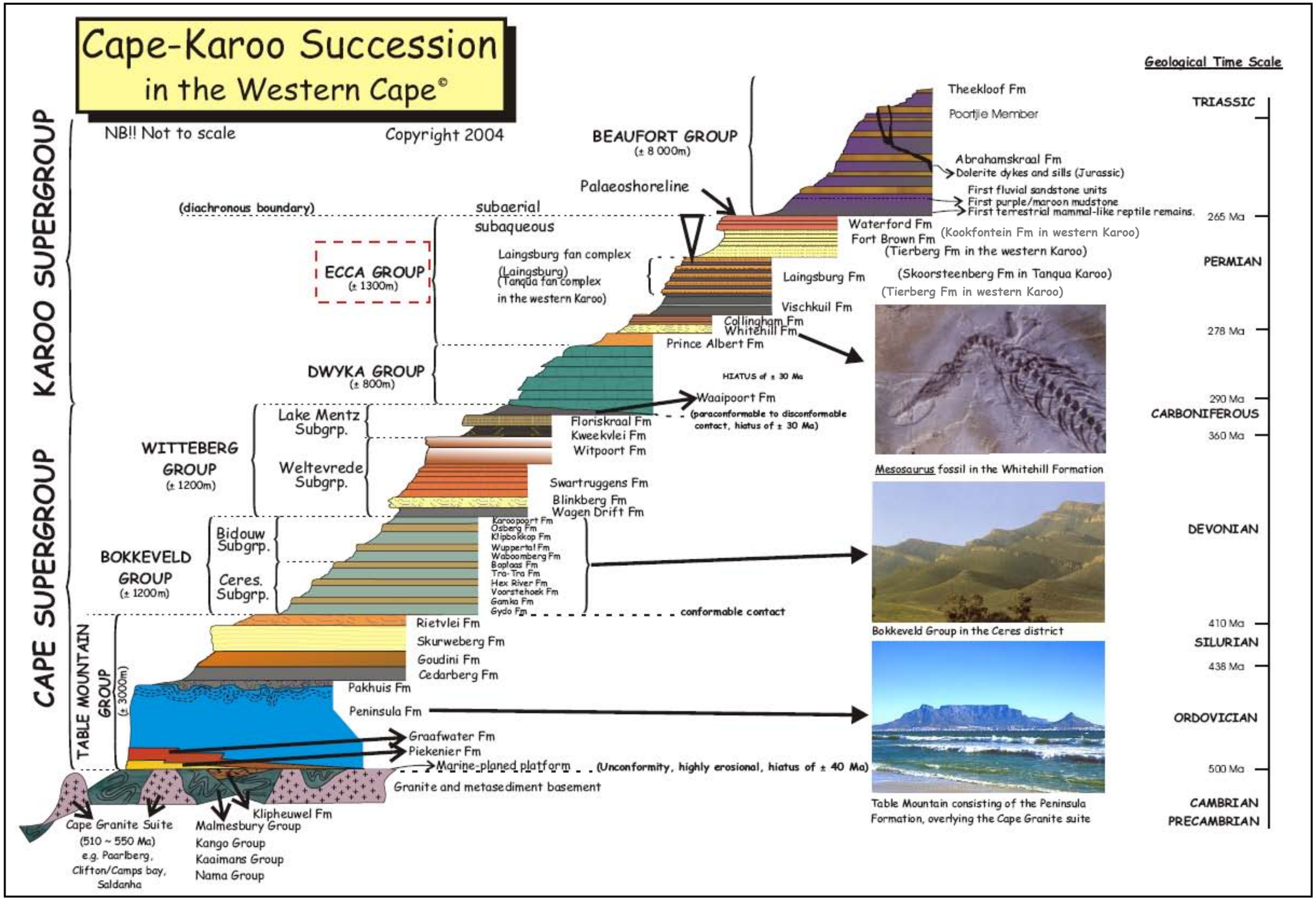

Figure 9: Illustration of the Cape-Karoo succession (from Wickens, 1994).

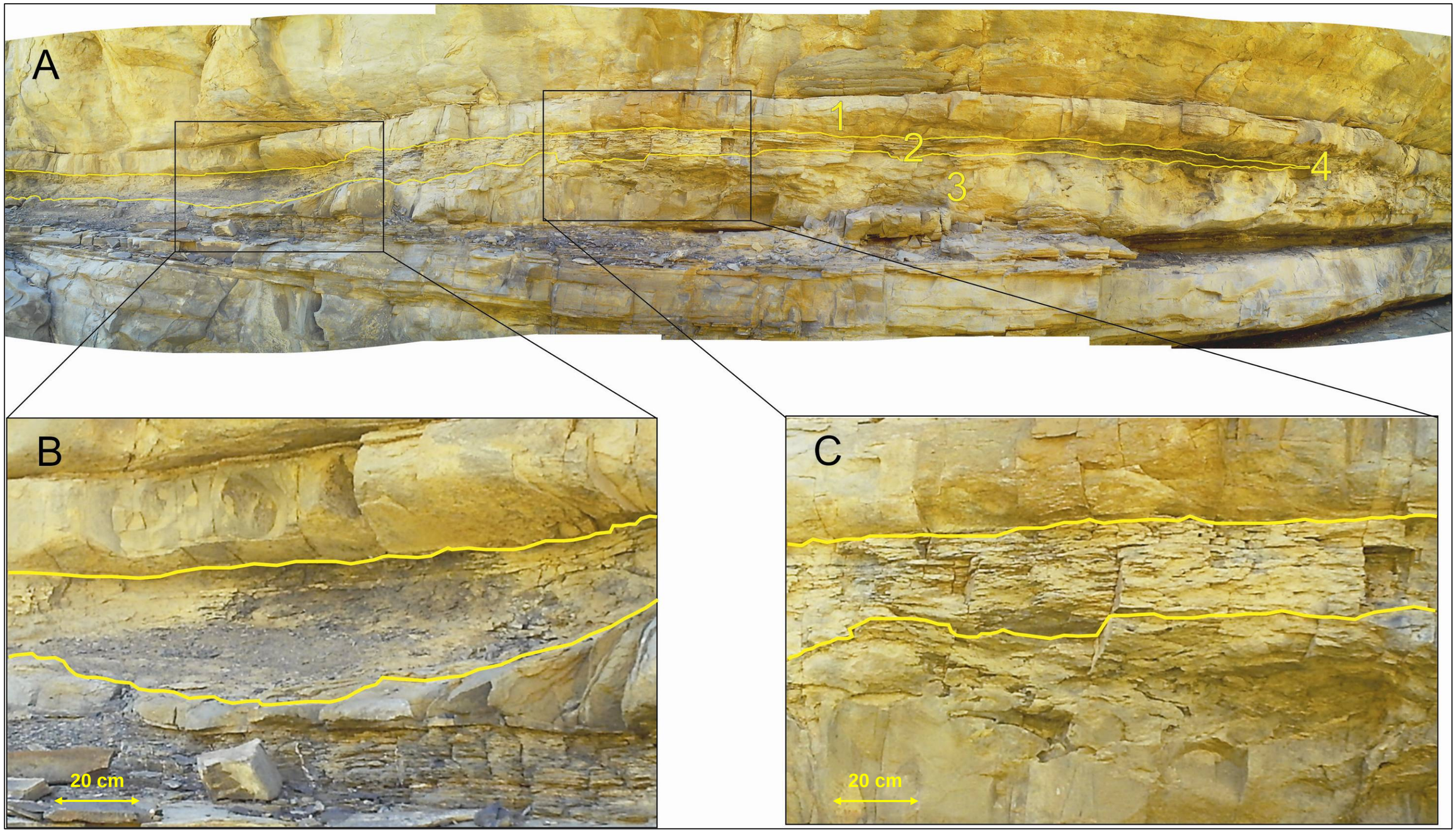

Figure 12: Panorama photomontage of the pinch out of the debritic part of a co-genetic bed (A) with two close-ups (B&C) of the same photographed at the Fan 2 type locality where it forms part of profile R00A (34H0399360/UTM6373789, on the farm Kleine Gemsbok Fontein 72). Image A further shows 4, the pinch-out of the debrite; 3, the underlying massive sandstone; 2, the debrite; and 1, the overlying sandstone. The outcrop is viewed towards the east.

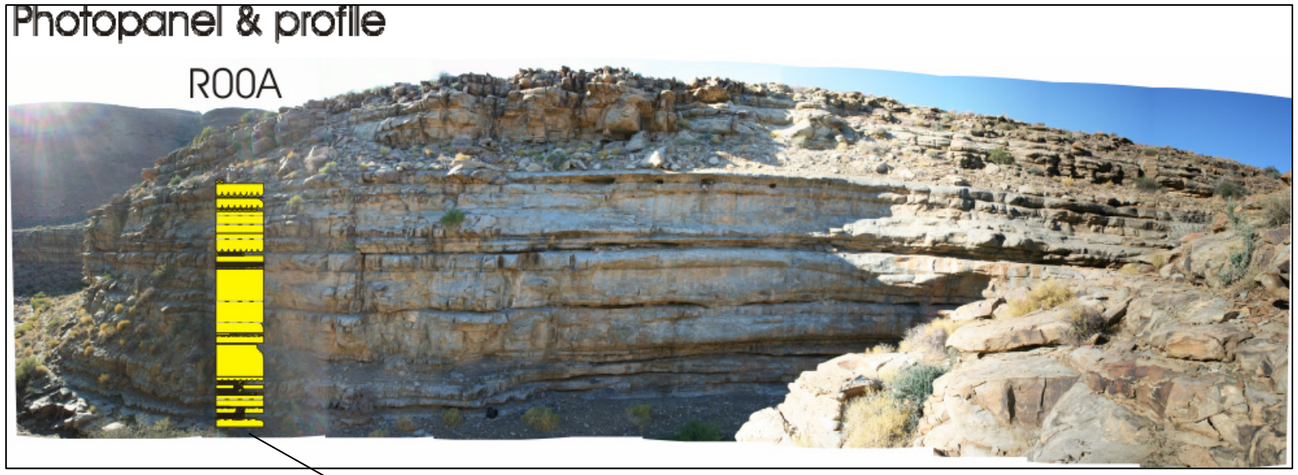

Figure 37: Vertical profile R00A (34H0399360/UTM6373789) compiled in CorelDraw format superimposed on its associated photopanel.

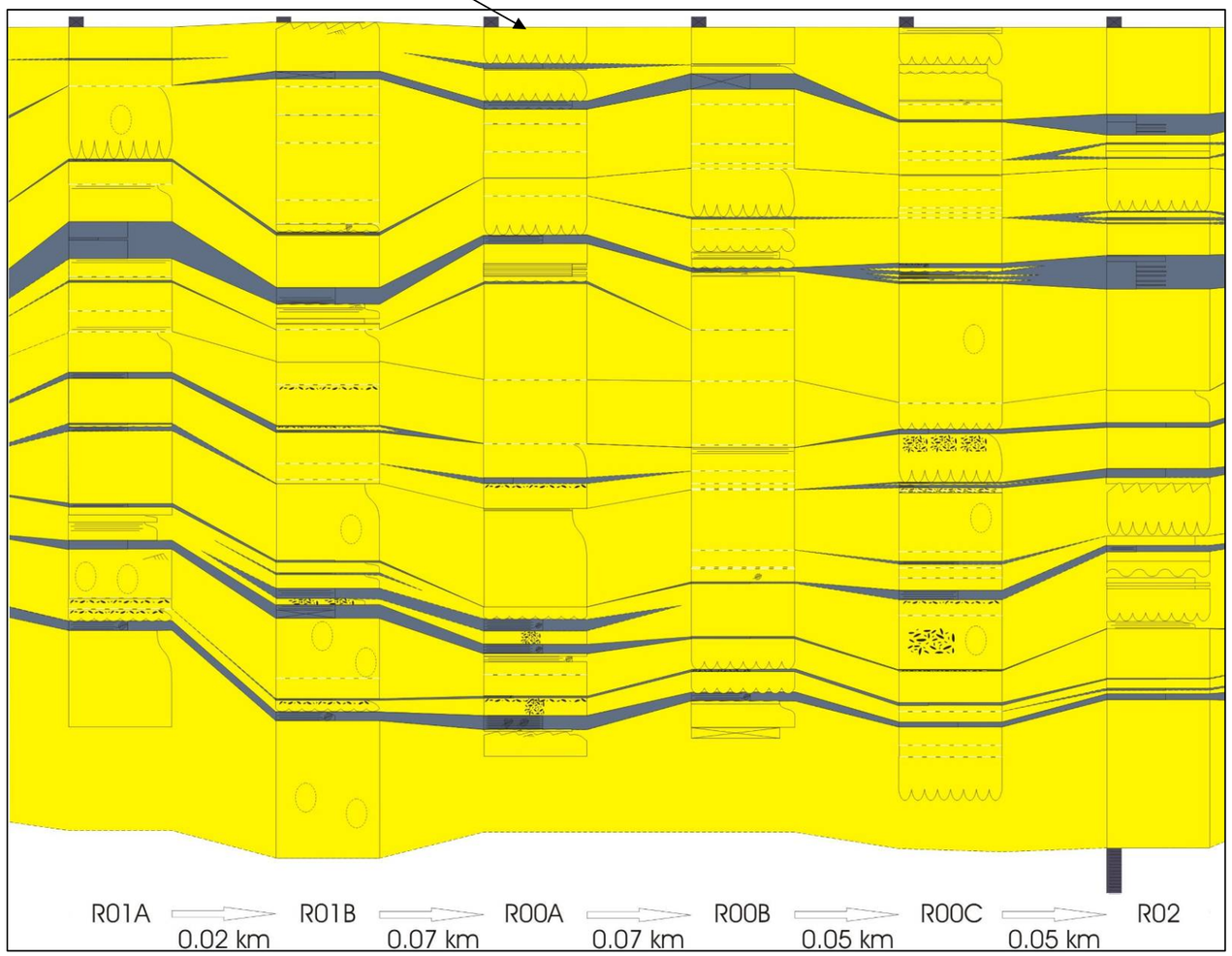

Figure 38: Vertical profiles R01A, R01B, R00A, R00B, R00C and R02 represented as a correlation panel in CorelDraw.

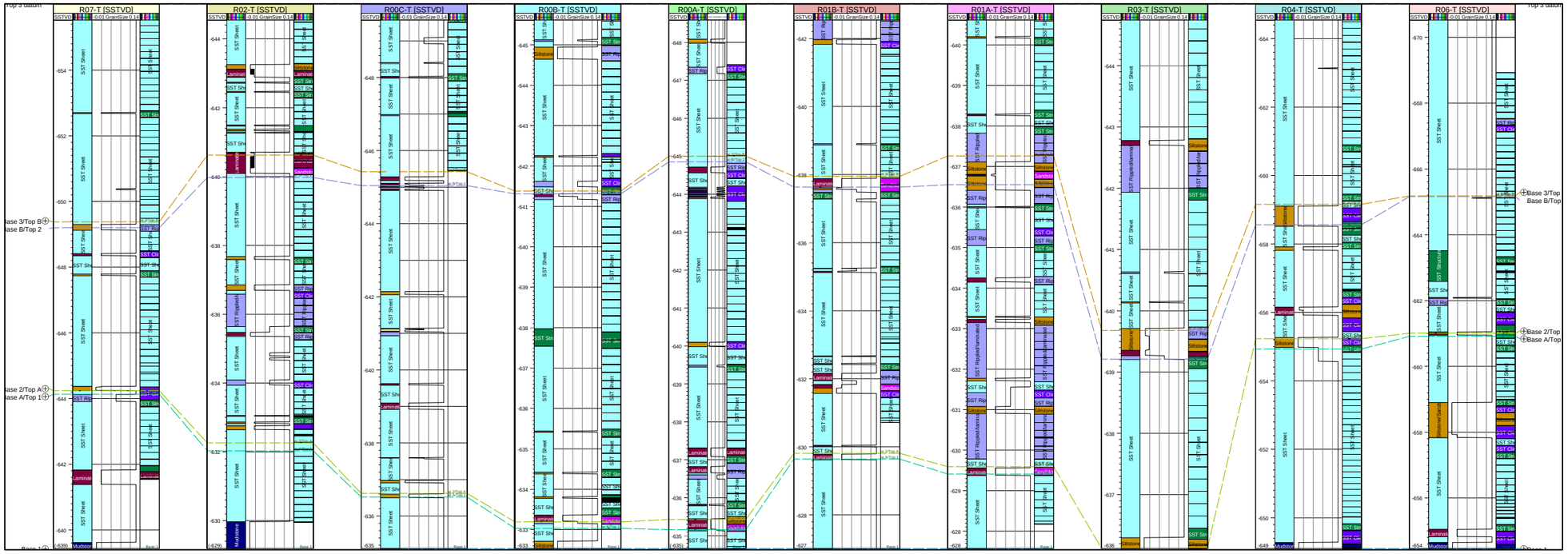

Figure 60: Correlation panel of profiles R00A to R07 using convergent interpolation and polygon A showing the original DSL facies on the left and the model-generated facies on the right.

Figure 61: Correlation panel of profiles R00A to R07 using sequential indicator simulation showing the original DSL facies on the left, grain size in the centre and model-generated facies on the right.

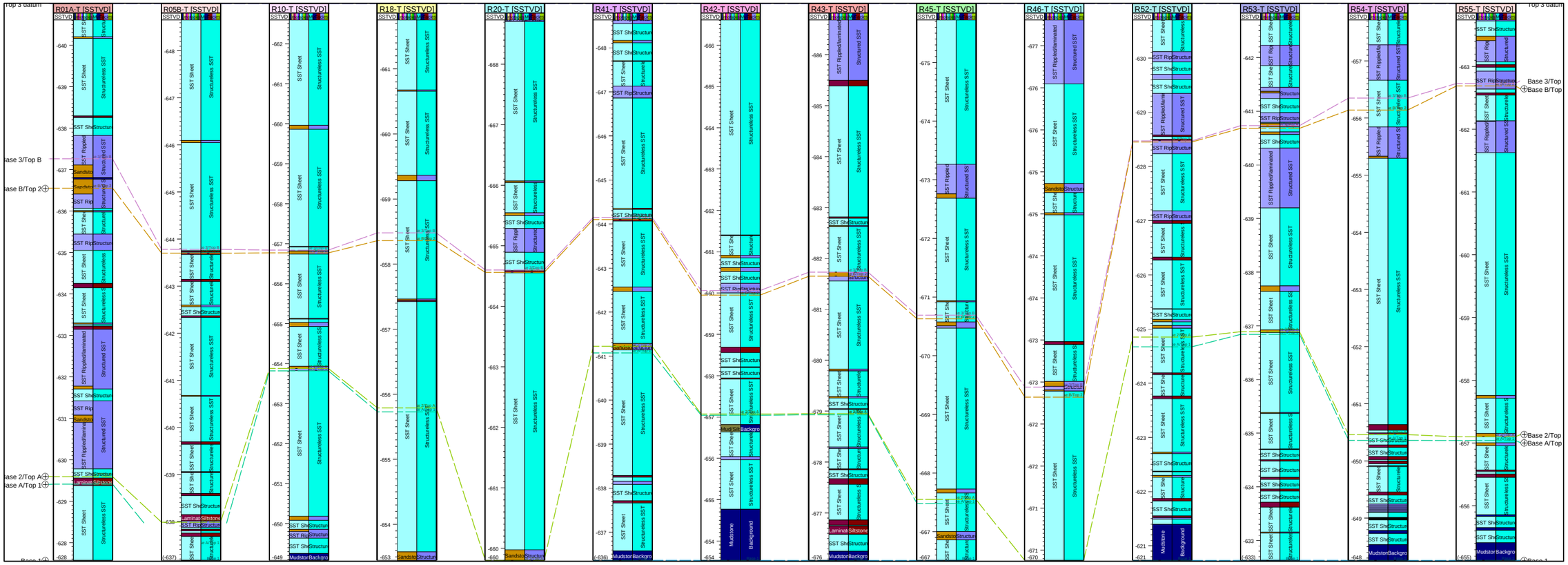

Figure 63: Petrel correlation panel generated along dip.

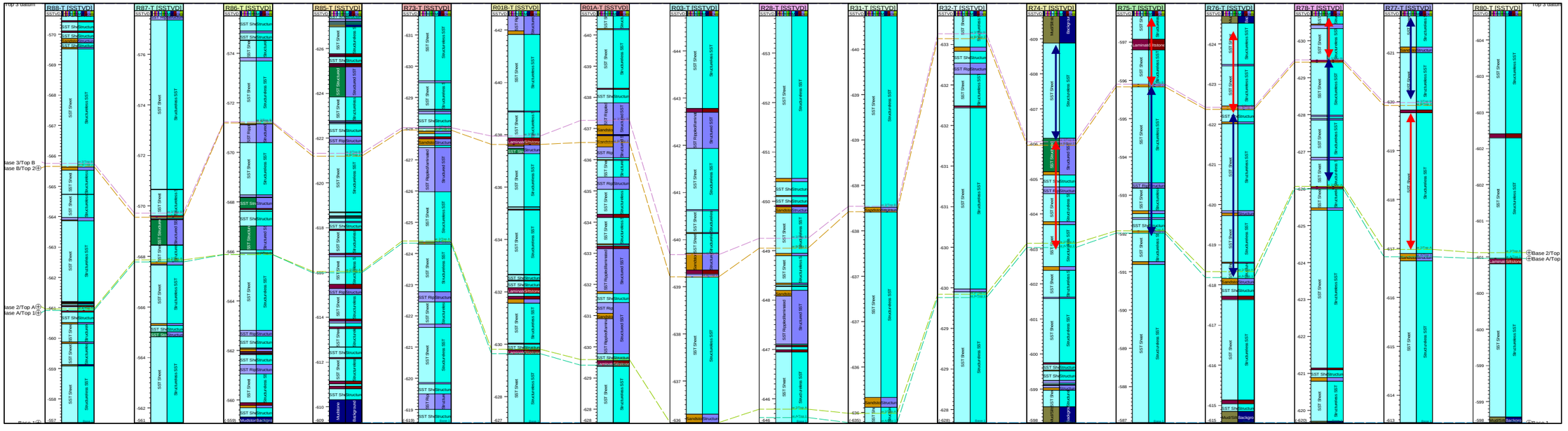

Figure 64: Petrel correlation panel generated along strike, illustrating compensational stacking with thickening lobe elements indicated by a blue arrow and thinning lobe elements indicated by a red arrow.

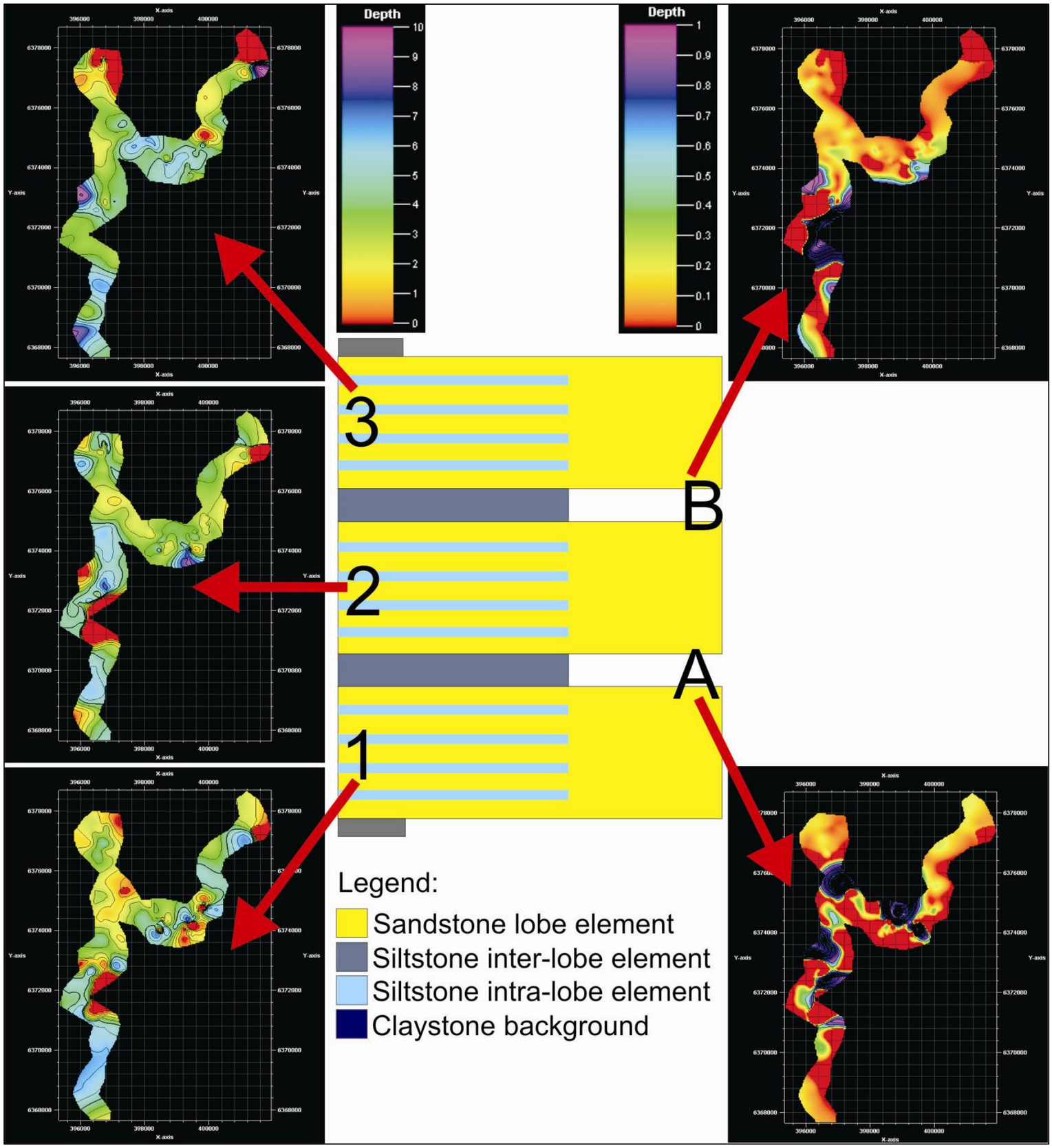

Figure 73: Isopach maps generated for sandstone-lobe elements 1, 2 and 3 and siltstone inter-lobe elements A and B. The thickness scale for the lobe elements is 0 – 10 metre. The thickness scale for the inter-lobe elements is 0 – 1 metre.

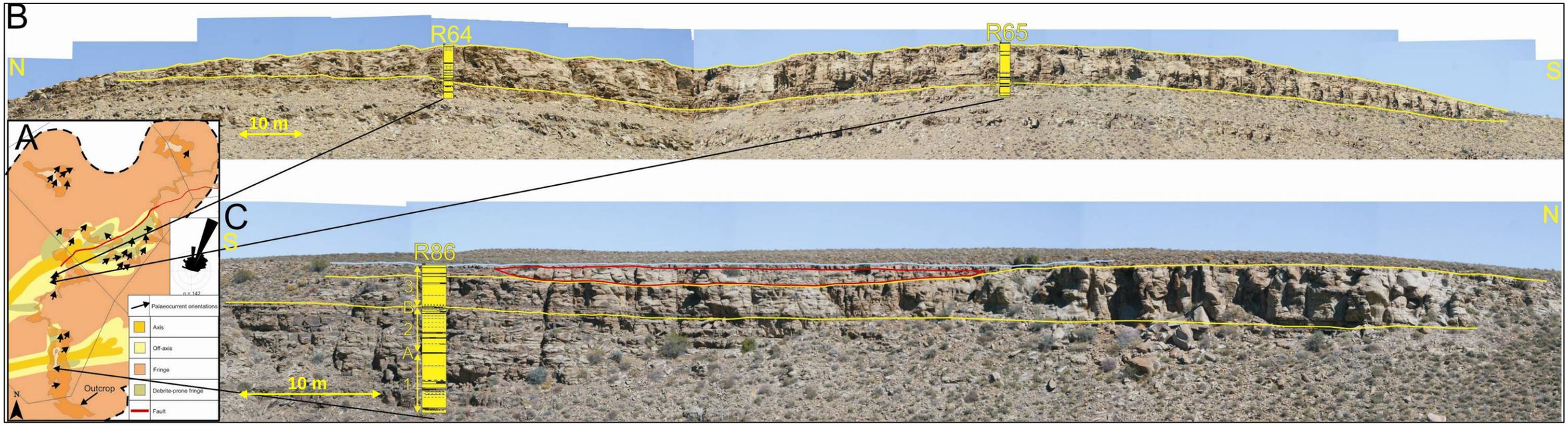

Figure 79: Image A shows the depositional model for Middle Fan 2 generated in this study.

Image B is a photomontage showing the positions of vertical profiles R64 (34H0396418/UTM6373257) and R65 (34H0396282/UTM6373117). It is viewed towards the east. The channel (outlined in yellow) can be seen to thin laterally to both the north and south. The sandstone beds in the channelised area thicken substantially towards the axis of the channel where they amalgamate to form a vertically stacked sandstone package. The lateral extent of the channelised area is 250 metres. The vertical scale equals the horizontal scale.

Image C is a photomontage showing the position of vertical profile R86 (34H0396326/UTM6368930). It is viewed towards the west. Two channel-fills (in yellow and red) can be seen. The channel-fill outlined in yellow comprises a sandstone bed that thickens laterally from south to north as the compactional drape probably obliterated the original channel shape. The channel-fill outlined in red thins laterally to the south and north. The sandstone bed indicated by the blue line is an overlying bed that retains the same thickness throughout. The lateral extent of the channelised area is 100 metres. The vertical scale equals the horizontal scale.

The outcrop locations of both the channels are on the farm Kleine Riet Fontein 88. The legend can be seen in Figure 78, page 74.

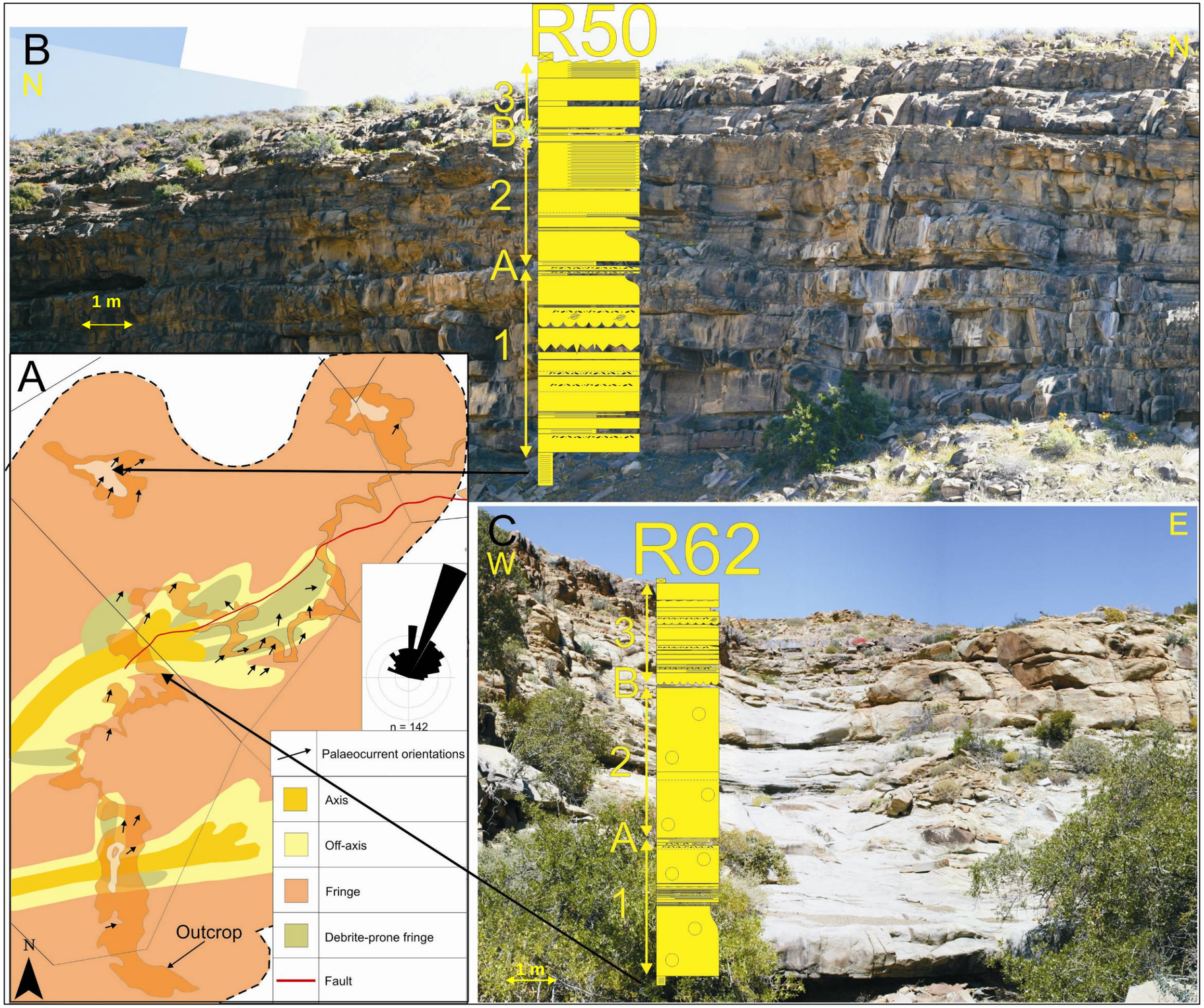

Figure 80: Image A shows the depositional model for Middle Fan 2 generated by this study.

Image B shows vertical profile R50 (34H0396732/UTM6376847) with layered sheets constituting the lobe elements. The sheets in this location are thinner than in the rest of the study area as each of the lobe elements are made up of numerous thin turbidite sandstone beds. This is due to the area being further away from the updip channelised area as it lies along the dip direction. The vertical scale equals the horizontal scale.

Note the parallel-laminated nature of beds in lobe elements 2 and 3, and the rip-up clasts at the base of sandstone beds in lobe-element 1.

Image C shows the position of vertical profile R62 (34H0396964/UTM6372859) with massive amalgamated sandstone beds forming the thick sandstone units. Very few siltstone beds are present. The vertical scale equals the horizontal scale.

Note the highly-amalgamated nature of the sandstone beds in lobe-element 2 and the profusion of secondary calcareous concretions. Rip-up clasts are found at the top of sandstone beds in lobe elements 1 and 3.

The legend can be seen in Figure 78, page 74.

Correlation panel 1

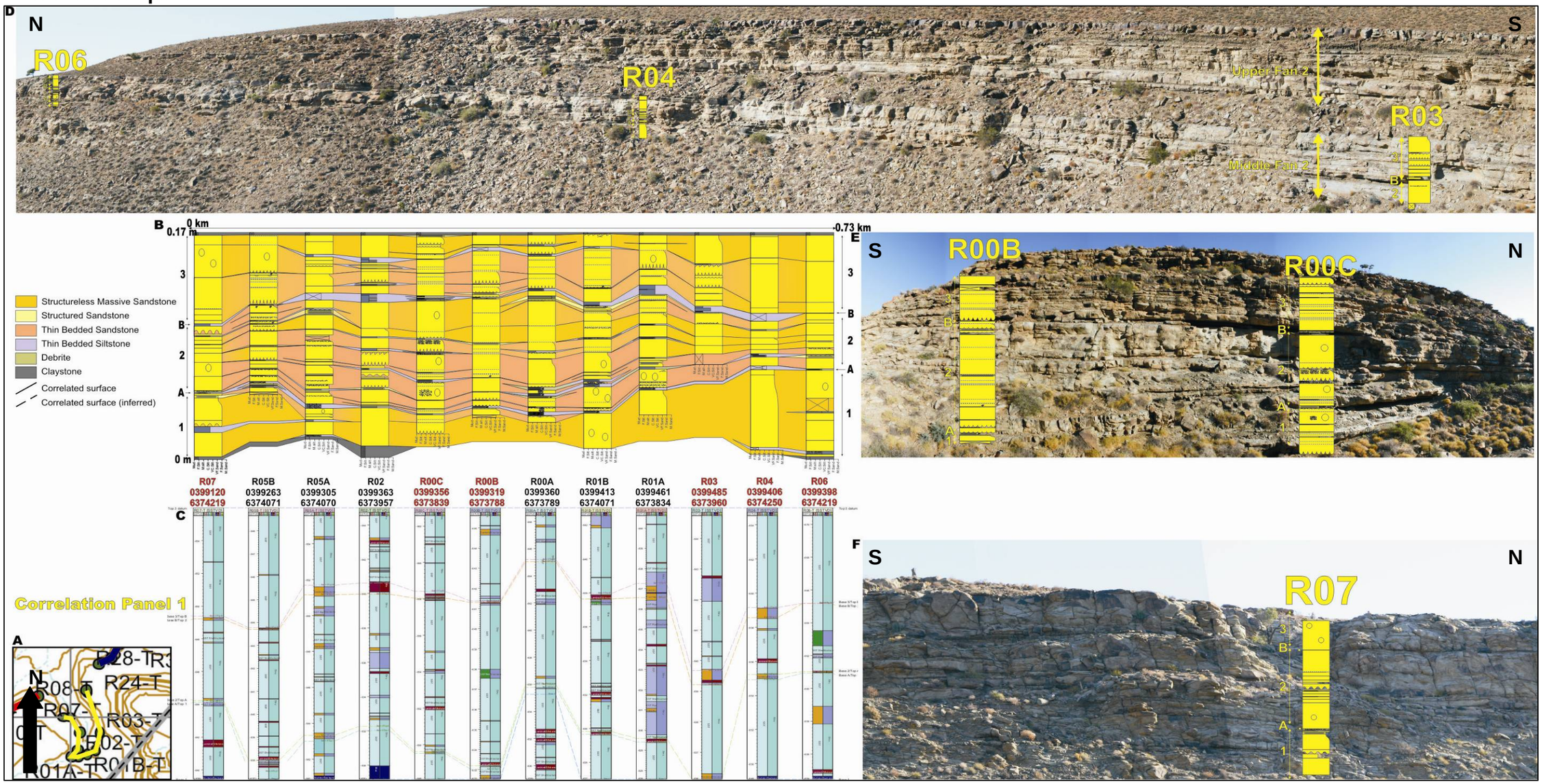

Figure 82: Correlation panel 1 of vertical profiles R06, R04, R03, R01A, R01B, R00A, R00B, R00C, R02, R05A, R05B and R07.

A: Location map of the profiles on the farm Kleine Gemsbok Fontein 72.

B: CorelDraw profiles were correlated to illustrate the largely massive sandstones of lobe-element 1, the thin-bedded sandstones of lobe-element 2 and the combination of the two facies in lobe-element 3.

C: Petrel profiles – note the dashed lines indicating the location of inter-lobe elements A and B throughout the panel, and in the process subdividing the lobe into lobe elements 1, 2 and 3.

D: The photopanel of R06, R04 andR03 illustrates that Middle and Upper Fan 2 are present in outcrop. Much of lobe-element 1 is obscured by scree or has been eroded away.

E: The photopanel of R00B and R00C illustrates the bedded nature of the lobe-element 3 and the poor exposure of lobe-element 1 due to obstruction by scree and sediment on the gully floor. Also note the amount of loading at the base of sandstone beds in this outcrop location.

F: The photopanel of R07 illustrates the amalgamated nature of the sandstone beds in lobe-element 3 and the top of lobe-element 2.

Correlation panel 2

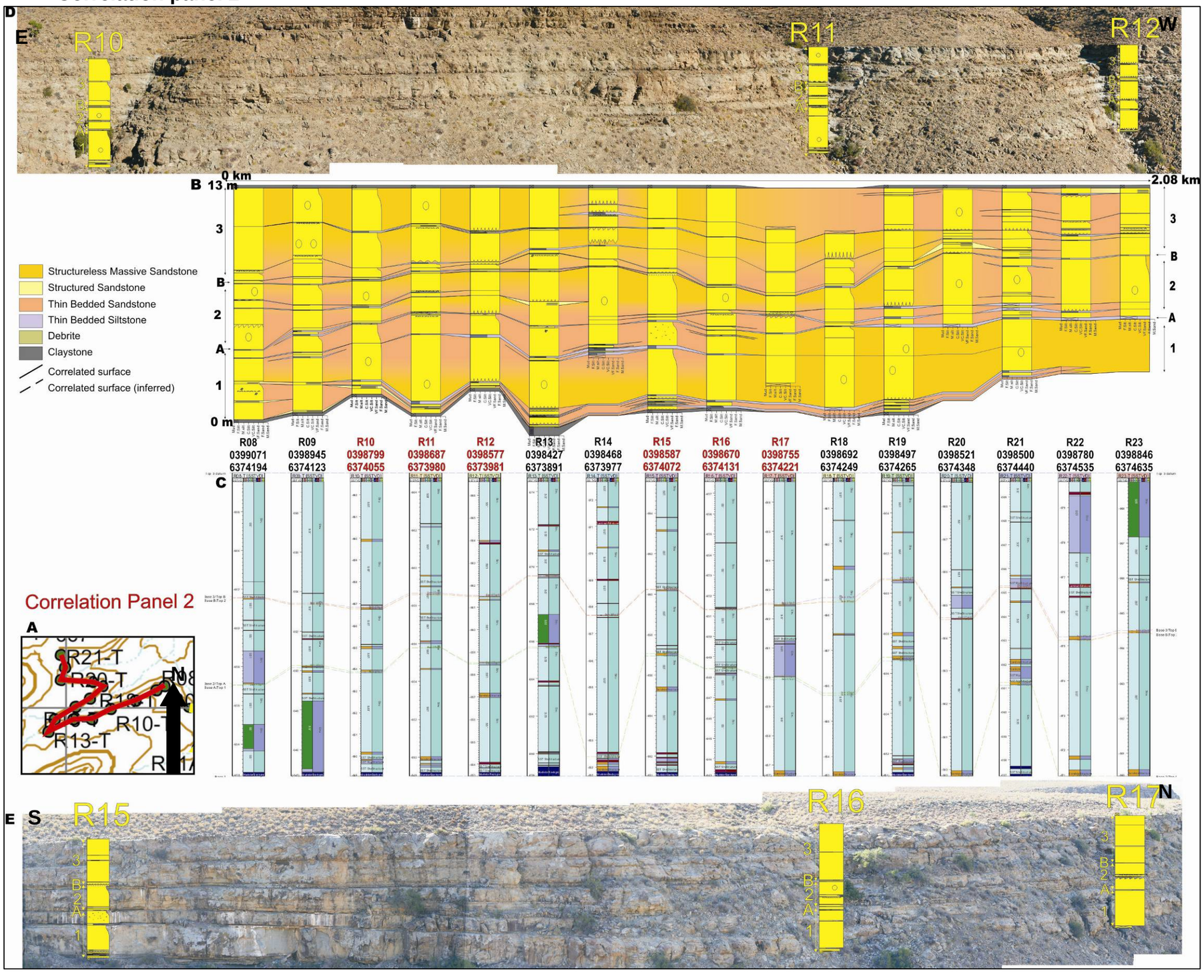

Figure 83: Correlation panel 2 of vertical profiles R08, R09, R10, R11, R12, R13, R14, R15, R16, R17, R18, R19, R20, R21, R22 and R23.

A: Location map of the profiles on the farm Kleine Gemsbok Fontein 72.

B: CorelDraw profiles were correlated to illustrate the variation from thin-bedded to massive sandstone from left (south-east) to right (north-west) across the panel for lobe-element 1, and the variation from massive to thin-bedded sandstone from left (east) to right (west) across lobe-element 3. Lobe-element 2 shows a combination of massive and thin-bedded sandstone. There is a zone of thin-bedded sandstones and siltstones at the bottom of lobe-element 1 (3 – 10 cm in thickness).

C: The Petrel profiles highlight the predominance of thin-bedded sandstones and siltstones at the base of lobe-element 1, and the location of structured sandstones (indicated in green and dark blue).

D: The photopanel of R08, R09, R10, R11, R12 shows the good quality outcrop enabling lobe elements to be traced out laterally. The photopanel is viewed to the south.

E: The photopanel of R15, R16, R17 shows the good quality outcrop, especially surrounding profile R15, enabling accurate lateral correlation. It also illustrates the bedded nature of the lobe elements in this location.

Correlation panel 3

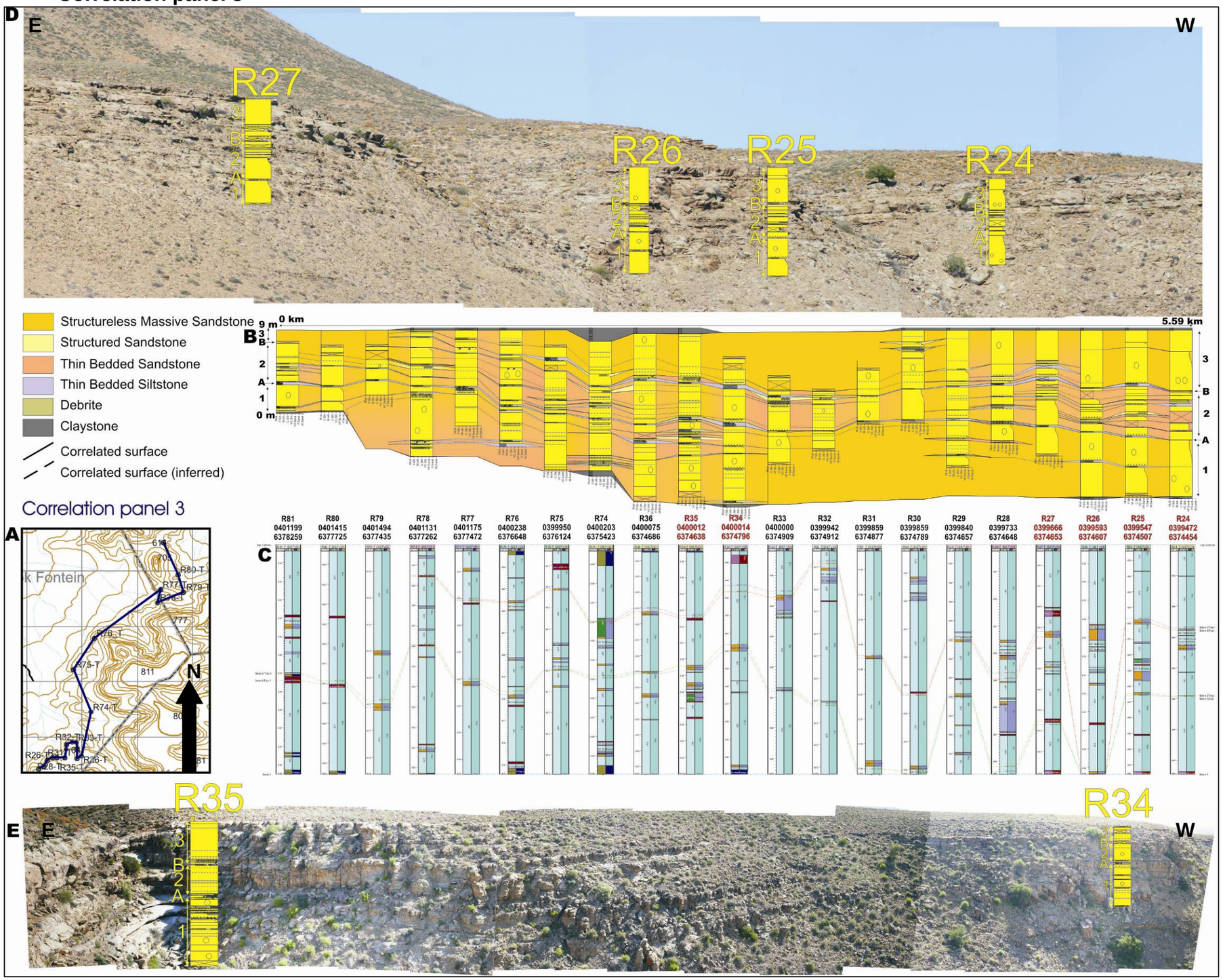

Figure 84: Correlation panel 3 of vertical profiles R81, R80, R79, R78, R76, R75, R74, R36, R35, R34, R33, R32, R31, R30, R29, R28, R27, R26, R25 and R24.

A: Location map of the profiles on the farms Kleine Gemsbok Fontein 72 and Los Kop 74.

B: CorelDraw profiles were correlated to illustrate the predominantly massive nature of the sandstone in lobe elements 1 and 3. It also highlights the structured, bedded nature of lobe-element 2. All three lobe elements thin significantly from right to left across the outcrop. This is equivalent to a thinning from west to east across the location map in the direction of the pinch out to the north-east. Also note the poor outcrop data available in profiles R31 to R33 due to erosion of lobe-element 3 and scree cover over lobe-element 1.

C: Petrel profiles – note the artificial exaggeration of the thickness of profiles R31 to R33 as Petrel stretches the available data of all the profiles to assume the same thickness.

D: The photopanel of R27, R26, R25, R24 illustrates some of the poorer outcrop quality encountered in the study area. Much of the outcrop is obscured by scree or eroded away. The photopanel is viewed towards the south.

E: The photopanel of R35 shows the typical good-quality outcrop in the back of a gully and the poor-quality outcrop outside of the gully, making correlation between profiles R35 and R34 more difficult. Note the ledge-like weathering of the massive sandstone in lobe-element 1 of profile R35.

Correlation panel 4

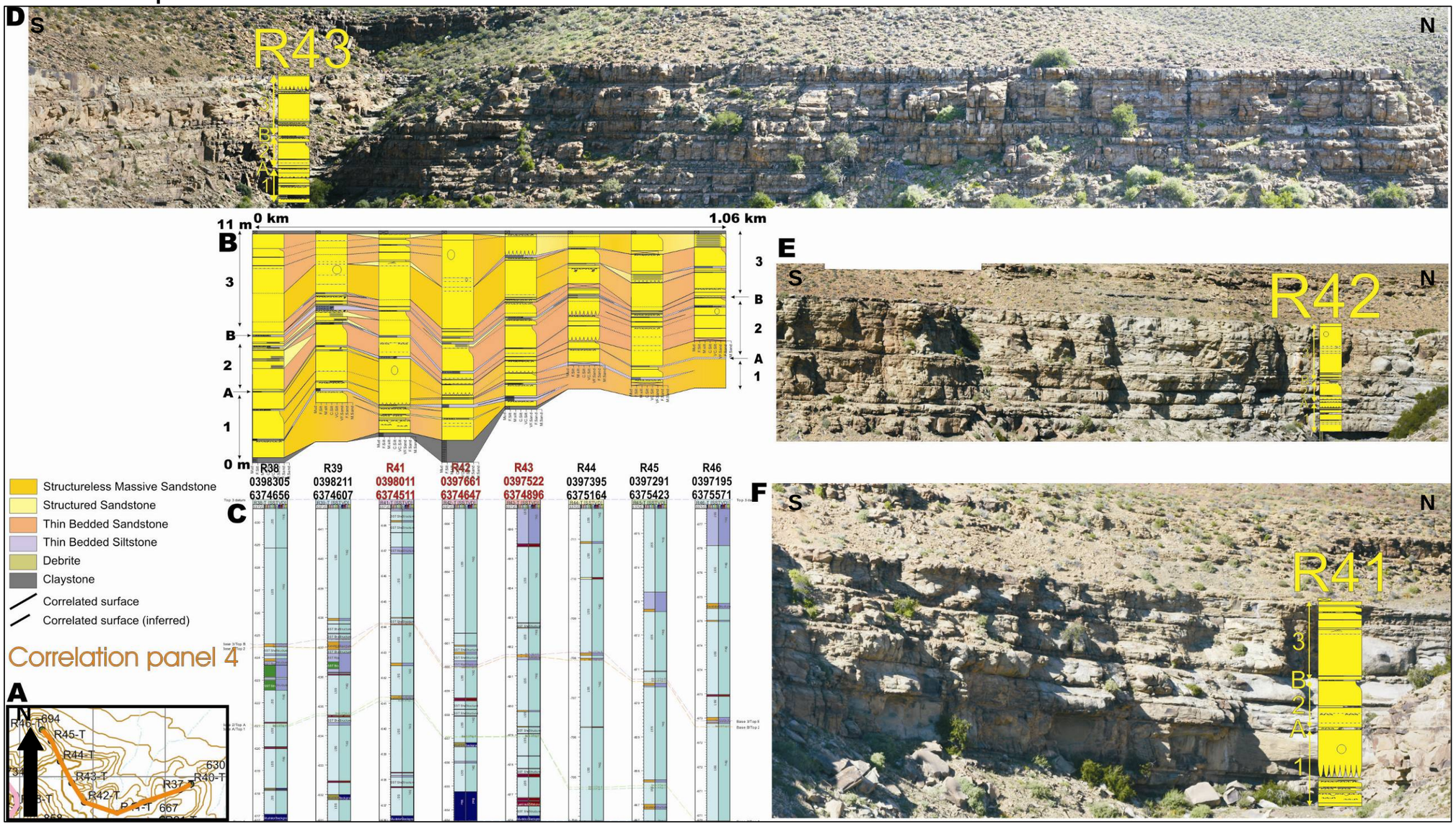

Figure 85: Correlation panel 4 of vertical profiles R38, R39, R41, R42, R43, R44, R45, and R46.

A: Location map of the profiles on the farm Kleine Gemsbok Fontein 72.

B: Correlated CorelDraw profiles illustrate the largely massive nature of the sandstone in lobe-element 3, the thin-bedded (3 – 10 cm) nature of sandstone in lobe-element 2, and the combination of the two facies in lobe-element 1. The correlation panel also illustrates the larger amount of siltstone intra-lobe elements present in this area.

C: Petrel profiles R38 and R39 mimic the thin-bedded nature of lobe-element 2.

D: The photopanel of R43 illustrates the excellent quality outcrop typical of the area covered by this correlation panel. Note the highly bedded areas interspersed with massive sandstone, and the lateral extent of lobe elements 2 and 3.

E: The photopanel of R42 highlights the thin-bedded sandstone nature of lobe-element 1, in comparison with F:, where the photopanel of R41 shows that only the lower half of lobe-element 1 is bedded, whereas the upper half is composed of massive sandstone. This change in facies occurs over a distance of 350 metres.

Correlation panel 5

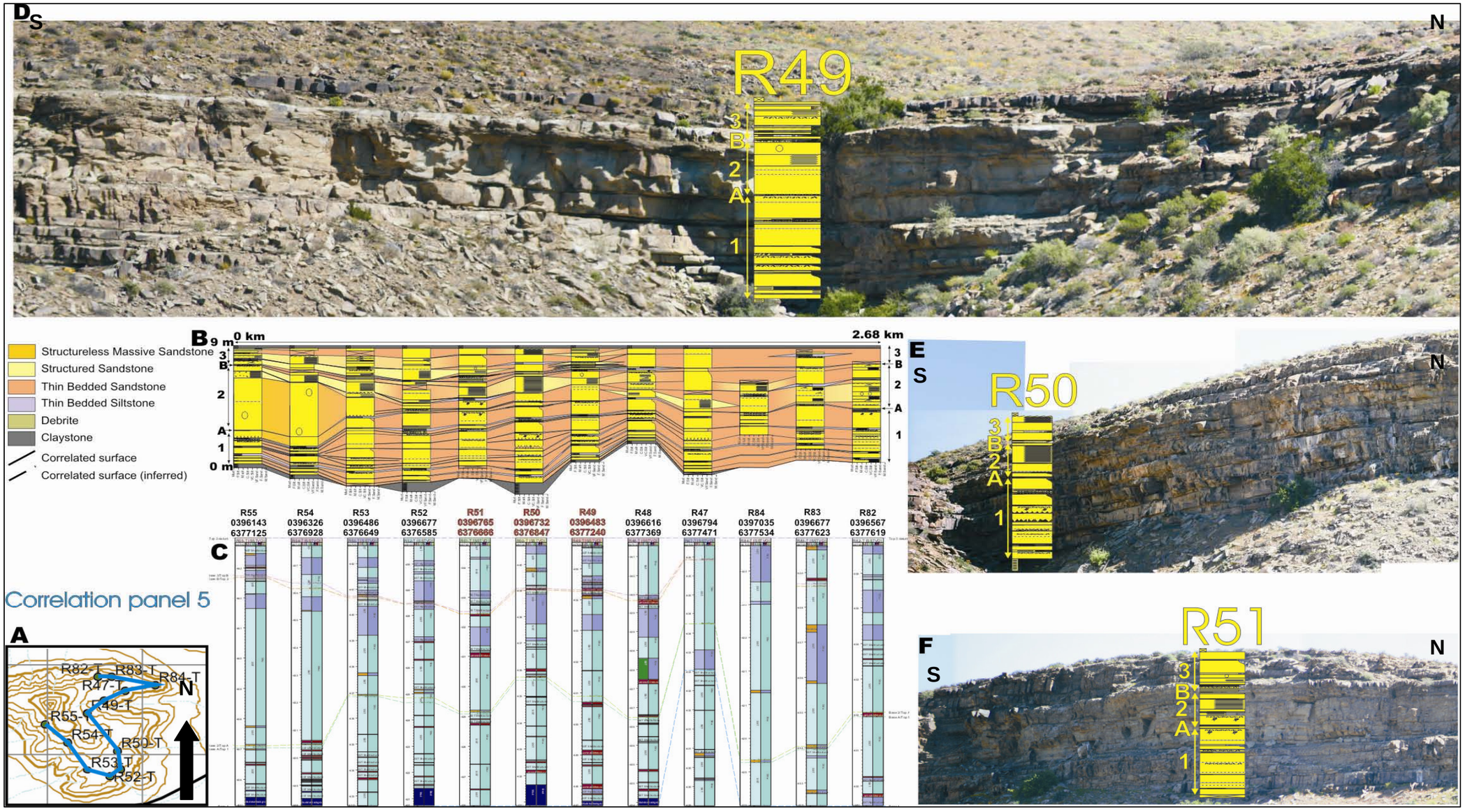

Figure 86: Correlation panel 5 of vertical profiles R55, R54, R53, R52, R51, R50, R49, R48, R47, R84, R83 and R82.

A: Location map of the profiles on the farm Kleine Gemsbok Fontein 72.

B: Correlated CorelDraw profiles illustrate the predominantly thin-bedded sandstone that predominates in this area. There are also many instances of structured sandstone, especially in lobe elements 2 and 3, which are predominantly composed of parallel-laminated sandstone. Note the large amount of siltstone intra-lobe elements.

C: The Petrel profiles in this correlation panel allow for the beds composed of structured sandstones to be clearly distinguished by their darker blue colour. They are commonly found in lobe-element 3 and the top half of lobe-element 2.

D: The photopanel of R49 shows the thin beds (3 – 10 cm) of lobe elements 1 and 3, and the amalgamated sandstones of lobe-element 3.

E: The photopanels of R50 and F: R51 illustrate the thin-bedded sandstones commonly found in this part of the study area. Note the parallel-laminated beds seen in lobe elements 2 and 3.

Correlation panel 6

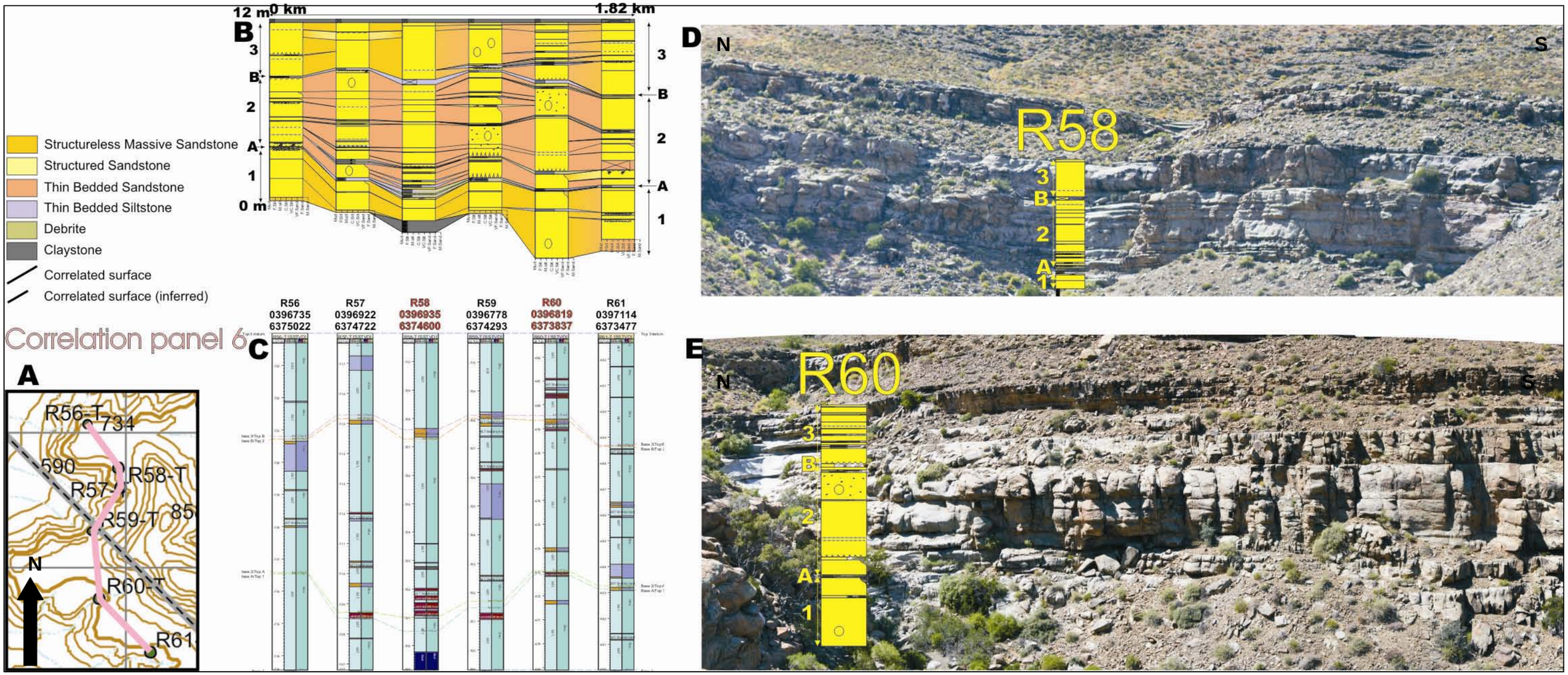

Figure 87: Correlation panel 6 of vertical profiles R56, R57, R58, R59, R60 and R61.

A: Location map of the profiles on the farms Kleine Gemsbok Fontein 72 and Kleine Riet Fontein 88.

B: Correlated CorelDraw profiles show that lobe elements 1 and 3 are largely composed of massive sandstone, but that it changes to thin-bedded sandstone to the right side (east side) of the panel. Lobe-element 2 is largely composed of thin-bedded sandstone, but changes to more amalgamated and massive to the right (south south-east) of the panel. This indicates a measure of compensational stacking between the lobes. Note the large amount of siltstone intra-lobe elements in lobe-element 2.

C: The Petrel profiles highlight siltstone inter-lobe element A (in red-brown) between lobe elements 1 and 2.

D: The photopanel of R58 illustrates the massive nature of lobe-element 3 in contrast with the thin-bedded nature of lobe-element 2 directly below it towards the left side (west) of the panel.

E: The photopanel of R60 illustrates the more thin-bedded lobe-element 3 and the more massive lobe-element 2 found to the right side (south south-east) of the panel.

Correlation panel 7

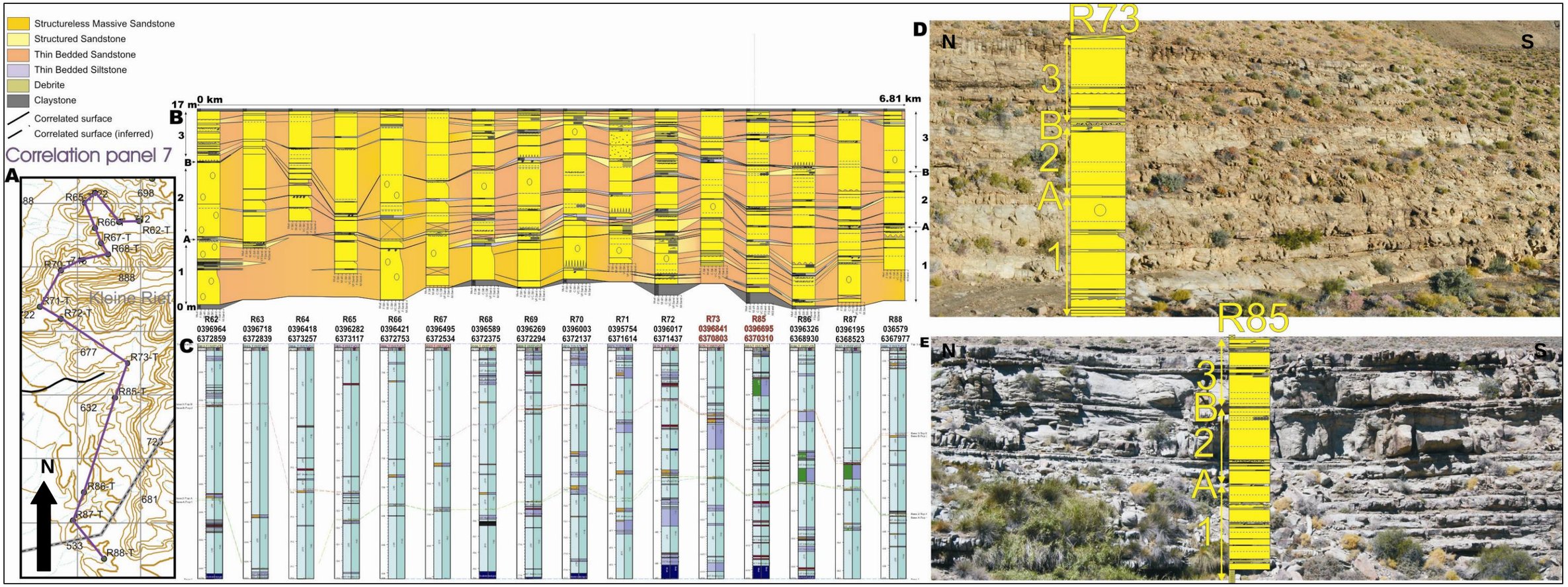

Figure 88: Correlation panel 7 of vertical profiles R62, R63, R64, R65, R66, R67, R68, R69, R70, R71, R72, R73, R85, R86, R87 and R88.

A: Location map of the profiles on the farms Kleine Riet Fontein 88 and Drie Fontein 87.

B: Correlated CorelDraw profiles illustrate the predominantly massive sandstone composition of lobe elements to the left (corresponding to north on the map) of the panel and predominantly thin-bedded sandstone to the right (corresponding to south on the map) of the panel. Profiles R64, R65 and R86 were measured in channelised areas. Note the significant thickening of lobe-element 3 from profile R64 to R65 and the thinning of lobe-element 2.

C: The Petrel profiles show the gradual change-over from massive to structured sandstone from left (north) to right (south) across the correlation panel.

D: The photopanel of R73 illustrates a combination of amalgamated massive sandstone in lobe-element 2 and the top of lobe-element 1, and thin-bedded sandstone at the base of lobe-element 1.

E: The photopanel of R85 illustrates good quality outcrop that highlights the thin-bedded nature of lobe-element 1 and the more amalgamated nature of lobe-element 2.

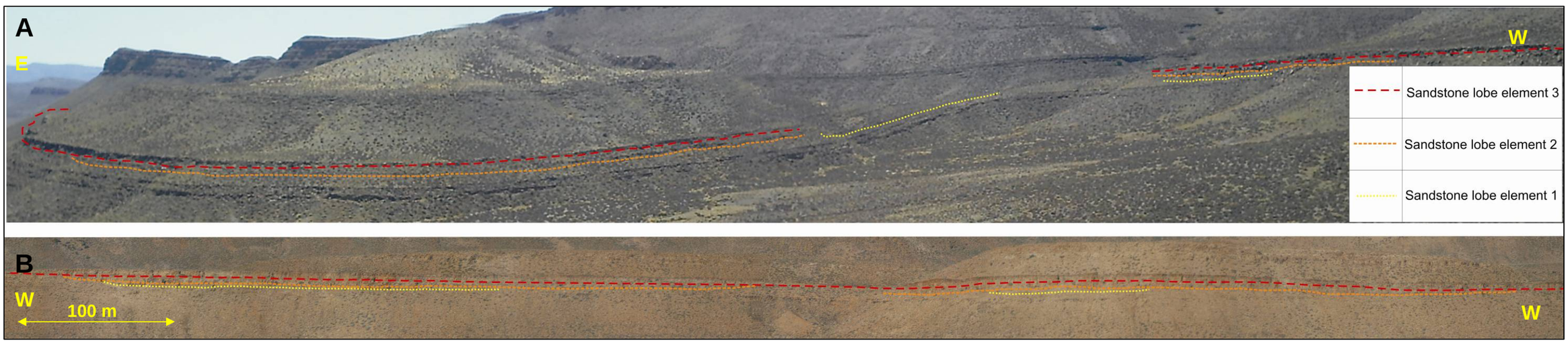

Figure 92: Panorama photomontage illustrating the pinch-out of lobe elements 1 (yellow), 2 (orange) and 3 (red) on the farms Los Kop 74 (Image A) in the north-east (down-dip) and the farm Drie Fontein 87 (Image B) in the south-southwest (up-dip). Lobe-element 1 pinches out first in both locations, followed by lobe-element 2, and finally by lobe-element 3.

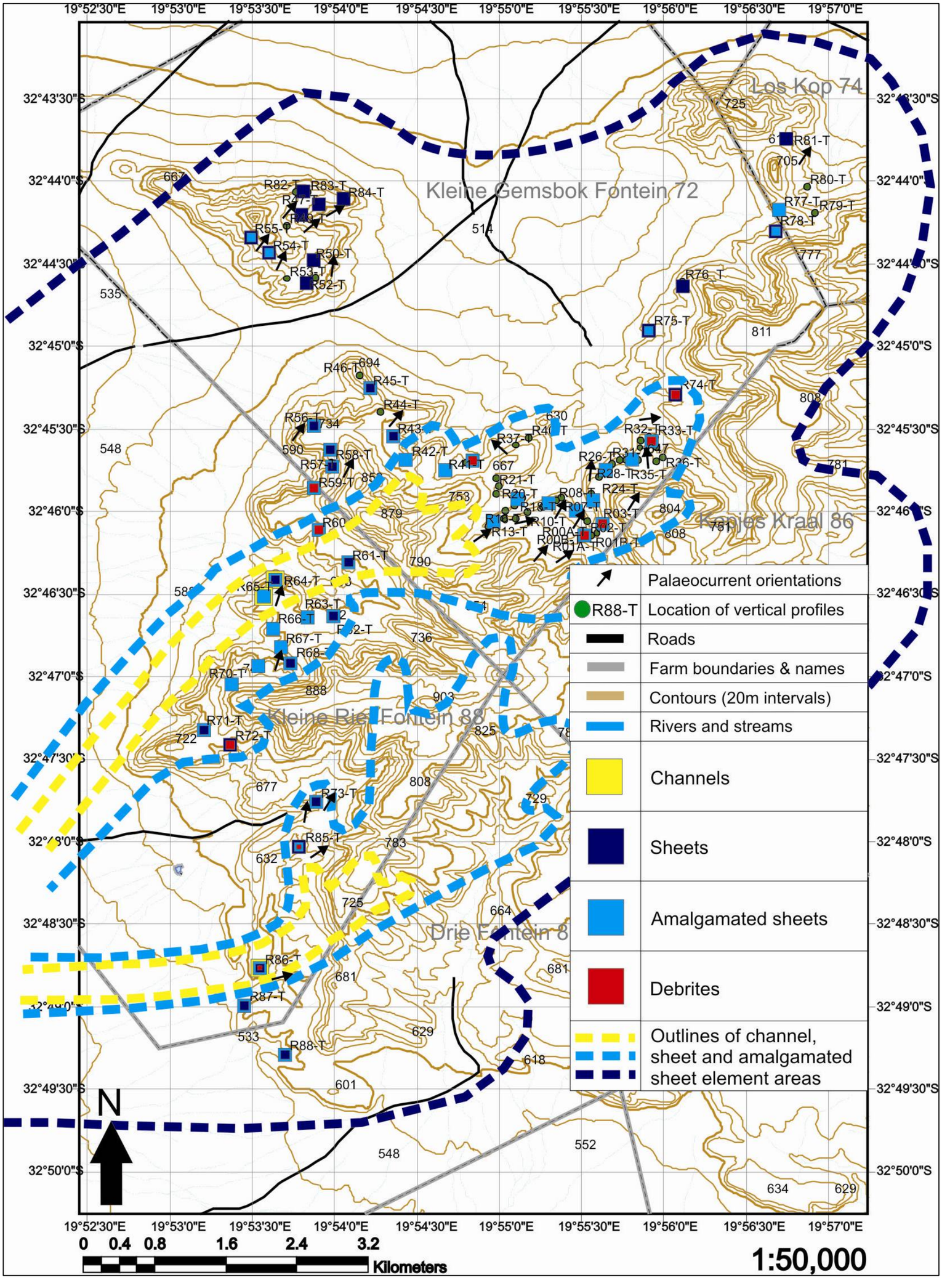

Figure 98: Depositional model for Middle Fan 2 generated using outcrop.

Geological reservoir modelling and process-based numerical modelling of deep-water distributive systems from detailed outcrop data:
examples from the Tanqua depocentre, South Africa

Hodgson, D.M.[1], Prelat, A[1]., Groenenberg, R.[2], Paulissen, W.E.2, Luthi, S.M.[2], Neethling, J.[3], Steyn, R.[3], Wickens, DeV.[3]

[1] Stratigraphy Group, Department of Earth and Ocean Sciences, 4 Brownlow Street, University of Liverpool, Liverpool, UK
[2] Department of Geotechnology, Delft University of Technology, The Netherlands
[3] Department of Geology, Geography, and Environmental Studies, Cnr Ryneveld and Merriman Streets, Stellenbosch, Western Cape, South Africa

A. Introducing the problem and the tools used

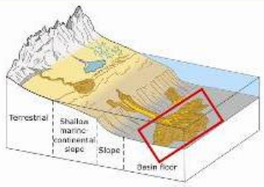

Terminal submarine fan lobes are distributive systems at the most down-dip depositional position of terrigenous sediment transported by gravity flows through basin margins. As such, they form an important, if cryptic, record of the interplay between climatic, eustatic and tectonic controls on the transfer of sediment from land to ocean. Distributive systems are dominated by depositional processes, although erosional processes are still important.

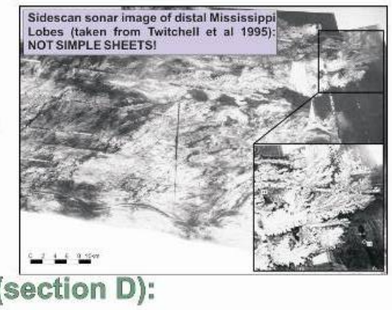
Sidescan sonar image of distal Mississippi Lobes (taken from Twitchell et al 1995): NOT SIMPLE SHEETS!

A1. Key questions:

On the shape, dimensions and geometries of lobe deposits (section B):
- What is the architectural hierarchy of elements in distributive systems?
- What is the depositional shape, dimensions and stacking patterns of lobe deposits?

On the prediction of the subsurface (section C):
- Can small-scale outcrop data be effectively imported and represented in 3D modeling software?
- Does the resulting output data remain true to the input data after upscaling of facies?

On the control on geometry and stacking patterns of the lobe deposits (section D):
- What controls the stacking of lobes and lobe elements?
- Are the stacking patterns and hierarchy identified at outcrop possible to simulate using a forward modelling approach?
- What is the interplay of autogenic and allogenic controls required to produce the lobe geometries, stacking patterns and volumes observed in the Karoo deposits?

A2. Tools for answering:

B. Geological model

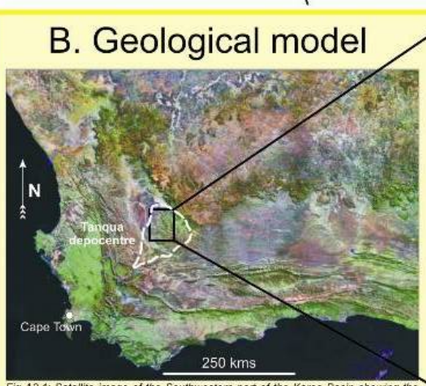

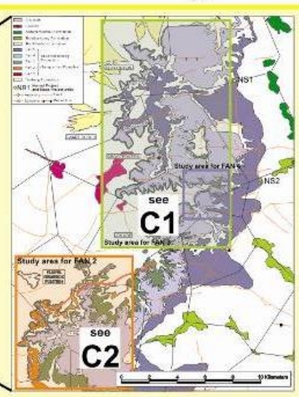

Fig A2.1: Satellite image of the Southwestern part of the Karoo Basin showing the location of the Tanqua Depocentre. Geological map of the Skoorsteenberg Fm. (adapted from Wickens 1994)

Outcrops of the Permian Tanqua depocentre were chosen because of their strike and dip continuity and good accessibility. They allow detailed study from bed to system scale.

The **Tanqua depocentre** is situated in the southwestern corner of the Karoo Basin and records sedimentation ins a retroarc forewland basin during the late Paleozoic and early Mesozoic. The Skoorsteenberg Formation (**~255 Ma; Fildani et al. 2007**), the focus of this study, consists of four basin floor fans and one lower slope to base of slope unit.

- **Fan 2** was studied to document the changes in stratigraphy and sedimentology towards a fan pinch-out within a distal fan setting *(MSc work of Rochelle Steyn in* **POSTER C2)**
- **Fan 3** was studied in its most distal areas (starting 15 km from frontal pinchout). The aim is to document the evolution, architecture and hierarchy of lobe deposits *(MSc work of Jaco Neethling in* ***POSTER C1****/ PhD work of Amandine Prélat in* ***POSTER B****.)*
- Two static reservoir models were built for **Fan 4** from 49 sedimentary logs and the NB2 boreholes *(MSc work of Wieske Paulissen in* ***Poster E****)*.

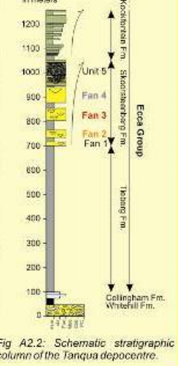

Fig A2.2: Schematic stratigraphic column of the Tanqua depocentre.

C: Reservoir modelling: *Petrel*

Petrel is used to build a 3D view of the studied geobodies. Fans 2, 3 and 4 were investigated and static reservoir models were built for each from sedimentary logs collected in the field:

- The data from 91 sedimentary logs were collected over the Fan 2 study area of 12 x 5 km. The data was used to generate a facies model for sandstone lobe- and siltstone inter-lobe elements for Middle Fan 2.
- The data from 72 sedimentary logs collected in the Fan 3 study area of 8 x 6 km was used to generate a facies model of 6 sandstone lobes .
- The data from 49 sedimentary logs in Fan 4 was also investigated.

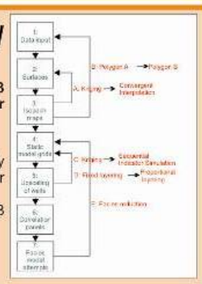

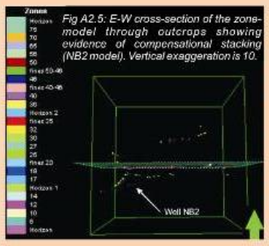

Fig A2.5: E-W cross-section of the zone-model through outcrops showing evidence of compensational stacking (NB2 model). Vertical exaggeration is 10.

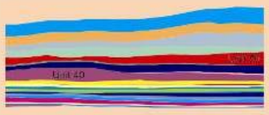

Isopach thickness maps:
Isopach maps are generated by subtracting surfaces from each other. Often, geobodies have a larger extent than the isopachs map boundaries. Generally, trends can be drawn when coupled with palaeocurrents.

Simple grids:
Grids were created to define a 3D frame of reference for the study areas using surfaces. The grid allows each of the lobes or lobe elements defined at outcrop to be described as a zone in Petrel. Each zone is further subdivided into layers to simulate internal variation. The zone models represent several levels in the hierarchy of the lobe complex, and may provide insights into the trends of the zones and their stacking patterns.

Facies Modelling:
Based on the upscaled well-logs containing facies and facies associations, facies distributions can be visualized in 3D. Correlation panels, a 2D representation, can illustrate the differences between input and output data.

D: Process-based modelling: *FanBuilder*

The aim is to test some of the concepual models derived from outcrop observations, and to try and constrain some of the input parameters that governed the flow of the turbidity currents and the depositional architecture observed in the ancient distributive system.

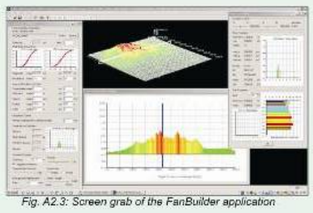

Fig. A2.3: Screen grab of the FanBuilder application

FanBuilder is a generic 3D process-based model capable of simulating the construction of fan stratigraphy by sequential turbidity-current events.

The core of the FanBuilder application patterns a process-based model capable of simulating turbidity-current flow behaviour and resulting sedimentation.

Input parameters are: initial topography, tectonic activity, grain size distribution, concentrations, magnitude and frequency of the flows.

The validation step is an essential step in the development of any model. During validation, the quality of the model is assessed and, preferably, quantified by comparing simulated results to a truth-case. Here, the truth-case is a laboratory experiment (Luthi, 1981), in which a mixture of water and suspended sediment flows out from a supply channel onto an expansion table (see Figure 4A) in the form of a small-scale turbidity current. The experiment itself may be considered to represent a downscaled version of turbidity currents that occur in nature, with a scaling of 1:103 to 1:105.

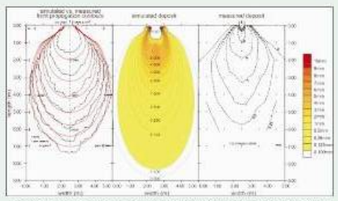

Fig. A2.4: Comparison of simulated flow behaviour and deposition vs. experimental data (Luthi, 1981)

B. INTERNAL ARCHITECTURE AND ORGANISATION OF TERMINAL LOBE DEPOSITS

B1. Hierarchy

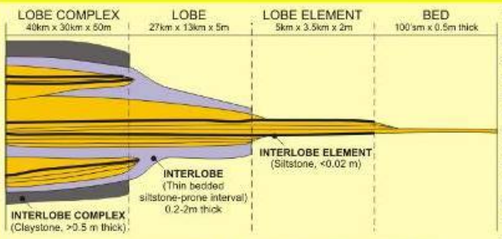

Fig. B1.1:Hierarchical element scheme for distributive systems based on Fan 3.

The development of a hierarchy of architectural elements that stack to construct a distributive deep-water system begins with identification of different types of bounding surfaces and/or fine-grained units.

- The fundamental building block in the stratigraphy of a distributive system is the ***bed***, which represents a single depositional event.
- One or more beds or bedsets stack to form a sand-rich ***lobe element***, which is separated from another lobe element by a locally eroded <0.02 m thick siltstone.
- One or more genetically related lobe elements stack to form a ***lobe***, which are typically 4-10 m thick, and several kilometres long and wide, and elongate in a downstream direction.
- Lobes are separated by fine-grained thin-bedded intervals that maintain similar facies and thickness for >8km in dip and strike sections, and are referred to as ***interlobes***.
- One or more genetically-related lobes stack to form a ***lobe complex*** (eg Fan 3). Lobe complexes are typically 30-60 m thick and bounded by 2-20 m thick claystones.

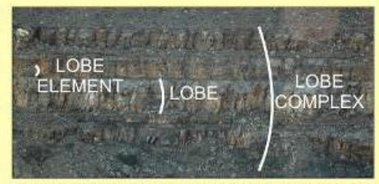

Fig. B1.2: Outcrop photograph of the Fan 3 showing the hierarchy of lobe element, lobe and lobe complex.

B2. Facies Distribution

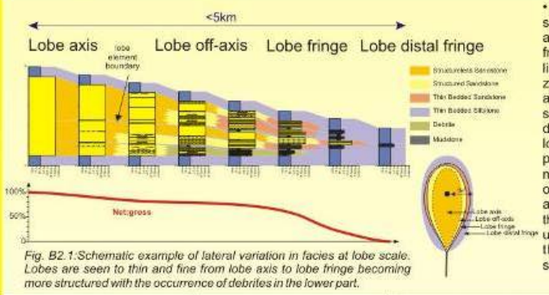

Fig. B2.1:Schematic example of lateral variation in facies at lobe scale. Lobes are seen to thin and fine from lobe axis to lobe fringe becoming more structured with the occurrence of debrites in the lower part.

- Facies transitions in lobes generally show an increase in bed stratification and tractional structures from axial to fringe settings. However, this is not a linear transition because multiple zones of increased bed amalgamation are identified along strike. In general, net:gross decreases from axis to fringe as the lobe thins. However, not all lobes pass from axis to fringe in the same manner. No clear pattern in the style of thinning has been documented, although we speculate that lobes that thin and fine are less confined by underlying topography than those that maintain a structureless sandstone facies.

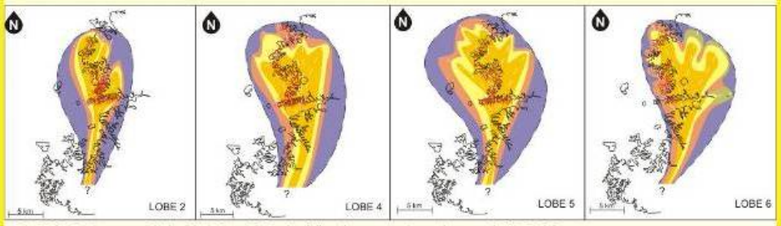

Fig. B2.2: Facies maps of lobes 2, 4, 5 and 6. Facies follow the same colour scheme as in Fig. B.2.2

Four broad environments of deposition in distributive systems have been identified for each element in the hierarchy: axis, off-axis, fringe, and distal fringe. Margin is avoided as this term has connotations with a confining surface.

- ***Axis settings*** are represented by >80% net: gross successions comprising amalgamated sandstone with local dewatering features, but no erosional confinement
- ***Off-axis settings*** are represented by 60-80% net: gross succession comprising stratified medium-bedded facies with Ta, Tab, and local Tc intervals, and some amalgamation. Some lenticular bedforms are identified here.
- ***Fringe settings*** are represented by 40-60% net: gross with medium- to thin-bedded successions of current ripple-laminated and/or bipartite and tripartite hybrid beds (linked debrites)
- ***Distal fringe settings*** are represented by <40% net: gross successions with thin-bedded very fine-grained sandstone and siltstone intervals that are commonly graded and ripple laminated.

B3. Shape

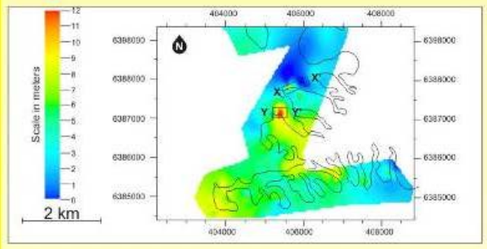

Fig. B3.1: ***Isopach maps*** were created from logged sections collected throughout the study area. Compilation of isopachs maps for each lobe and interlobe allow analysis of thickness variation, and construction of isopach maps.

Lobes are not simple radial bodies thinning evenly from the ceontroid (volumetric centre) as in an ellipsoid.
Lobe 2, for example, in distal reaches is characterised by abrupt changes in thickness across strike.

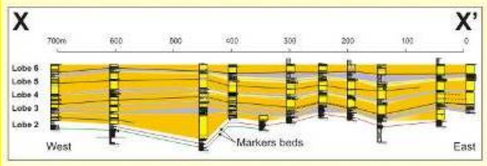

Fig. B3.2: **XX'** Lobe 2 thins from 3 m in the west to 0.1 m and then thickens back to 3 m moving east along strike. The cross-sectional geometry of this feature at outcrop is channel-form (base concave-up). Underlying marker beds are not truncated and follow the concave-up base of the lobe.

Fig. B3.3: **YY'** Up dip (500 m to the SW) along the same finger, Lobe 2 thickens to 14 m with a concave-up basal surface. Changes in thickness are abrupt and perpendicular to flow direction. Lobes that overlie the fingered basal lobe display minimal thickness variations.

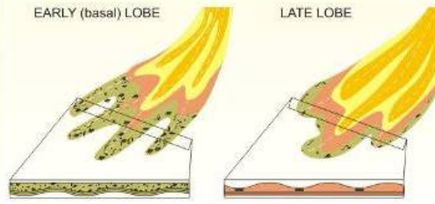

Fig. B3.4:Cartoon of early and late lobe and cross section through distal positions.

The pinchout pattern of Lobe 2 described above has a multiple finger-like expression. A similar pattern has been identified in basal lobes in Fan 3 in the Klipfontein area (lobe 4, this study), Fan 2 (Rozman 2000) and Fan 4 (Bouma and Rozman 2000). ***This finger-like pinchout pattern is particularly evident in basal lobes***, and indicates that the map view shape of lobes is not as smooth and radial as previously envisaged but can be much more irregular across strike. In contrast, the lateral fringe of lobe 6 is smooth and is parallel to the direction of thinning of the lobe, oriented N165. Away from its western fringe, lobe 6 thickens consistently at 2m/km.

B4. Stacking patterns

Local compensational stacking patterns

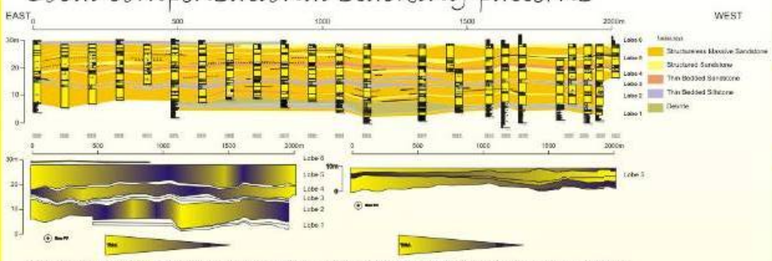

Fig. B4.1: A. Correlation panel of the Grootfontein south outcrop (strike section). B and C. Schematic correlation panels highlighting compensational stacking pattern of lobes and lobe elements.

- At outcrop, the compensational stacking of lobes is most apparent in strike orientated sections and can be demonstrated along a 2 km strike section in the Grootfontein area by the thickening and thinning patterns of lobes (2, 4 and 5).
- The maximum depositional relief is calculated by assuming that thickness change is due to seabed topography, and these estimates are presented as angles.
- From east to west, lobe 2 thins from 7.8 m to 4.2 m over 700 m (angle of 0.29°), thickens back to 10 m in 500 m (angle of 0.66°) and, at the western end, thins to 6.7m in 600m (angle of 0.32°). Locally, lobe 4 is thickest overlying the thinner parts of lobe 2, and thins from 5.4 m to 3.2 m over 1000 m to the east (angle of 0.13°). Finally, lobe 5 has two loci of thickening situated at either end of the panel and thickens from 6 m to 9 m in 1000 m towards the east and the west (angle of 0.17°).

Fig. B4.2: Diagram of compensational cycles after Mutti and Sonnino, 1981. Scale is indicative.

Planform stacking patterns

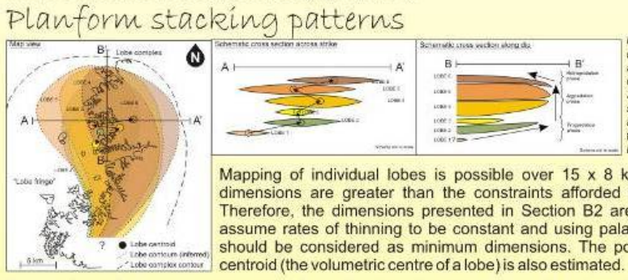

Fig. B4.3: Geometry of lobes within Fan 3 and stacking patterns of Lobes 2 to 6. Schematic cross section across strike and and along dip through the 6 lobes of Fan 3

Mapping of individual lobes is possible over 15 x 8 km, but a lobe's dimensions are greater than the constraints afforded by the outcrop. Therefore, the dimensions presented in Section B2 are estimates that assume rates of thinning to be constant and using palaeocurrents, and should be considered as minimum dimensions. The position of a lobe centroid (the volumetric centre of a lobe) is also estimated.

Nevertheless, the outcrop constraints indicate that the lobes are elongate in a down-dip direction with dimensions of several kilometres in length and width. Isopach maps, generated from logged thicknesses of lobes show a specific volume, position, and shape for each lobe within the field area.

B5. Dimensions

Methodology:

2D data, such as the lengths of surfaces, beds, bedsets, or 'shales', can be extracted easily from outcrop panels, but need to be reoriented from their outcrop lengths to be tied to local palaeocurrent directions.

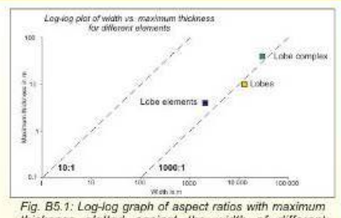

Fig. B5.1: Log-log graph of aspect ratios with maximum thickness plotted against the width of different architectural elements from Tanqua.

Key conclusions:

- Interlobe low permeability intervals (thin-bedded fine-grained facies) were deposited as a blanket over lobes to form significant barriers to vertical fluid flow that are cut out locally
- Bed thickness distributions form segmented power laws, which is related to bed amalgamation and lobe element confinement
- Width to length ratios show a linear relationship across the hierarchy of lobe components (Fig. B2.2.)
- A non-linear relationship exists between lobe element thickness and lobe element area, which indicates the presence of a process that limits lobe element thickness to <3m (Fig. B2.3.)
- Aspect ratios (width to thickness) of lobe elements, lobes, and lobe complexes are comparable (1000:1)
- Estimates of typical turbidity current volumes and number of beds that comprise lobe elements have been calculated and used to help constrain process-based numerical models (Poster D)

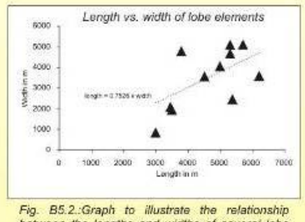

Fig. B5.2.:Graph to illustrate the relationship between the lengths and widths of several lobe elements identified in the Tanqua depocentre.

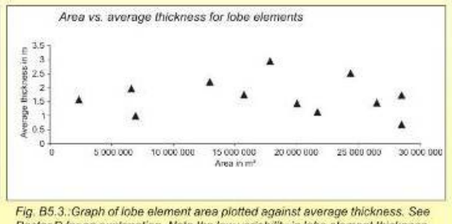

Fig. B5.3.:Graph of lobe element area plotted against average thickness. See Poster D for an explanation. Note the low variability in lobe element thickness, but wide range of lobe element area.

C. RESERVOIR MODELLING AND SUBSURFACE APPLICATION

Why geological reservoir modelling?
Modelling allows the visualisation of subsurface data in 3D that would not normally be visible in seismic data. Lateral facies variations is highlighted by the process, making the simulation of fluid flow possible. Digital outcrop models (DOM) provide a means to capture quantitative 1D, 2D ,and rarely 3D, data collected at outcrop.

1. Input data: vertical profiles measured in the study area includes information on sedimentary structures, architectural elements, bed thickness, facies, etc. This data can be visually represented as sedimentary logs and correlation panels in CorelDraw to highlight variation in stratigraphy, architecture and facies distribution.

2. Output data: input data is imported and manipulated in Petrel to build a 3D representation of the 2D outcrop data. The accuracy of the representation is dependant on the efficacy of the outcrop data for use in modelling software.

The work presented below forms part of theses by Jaco Neethling (C1) and Rochelle Steyn (C2), University of Stellenbosch.

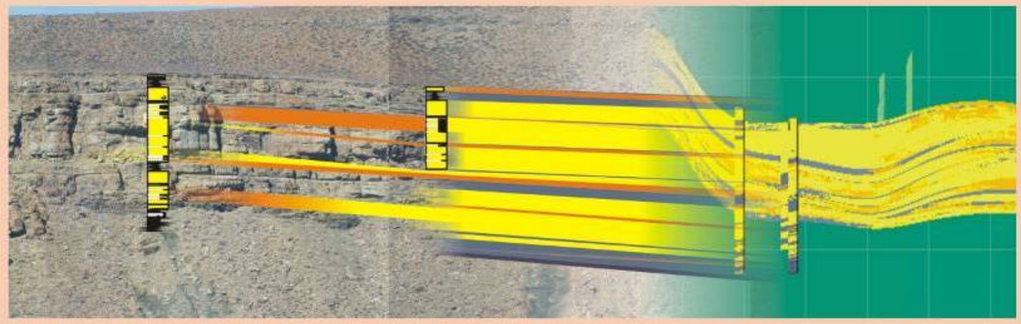

C1. lobe complex axis (Fan 3)

Outcrop observation

Outcrops of the **Fan 3 lobe complex** in medial axial position show a slightly different pattern to the outcrops studies to the north (Poster B). Lobe 3 is not present, and two additional lobes are present beneath Lobe 1. Lobes 2, 4 and 5 can be divided into **Upper** and **Lower lobe elements**, each exhibiting significantly different behaviour. For instance, Upper Lobe 5 pinches out 4 kilometres before Lower Lobe 5, and has a different palaeoflow direction. The outcrop below (Fig C1.1) represents the **southern Gemsbok valley**. Beneath are two correlation panels, one created in **CorelDraw** and the other a **Petrel** generated panel, both indicating facies variation across the 3800km long outcrop.

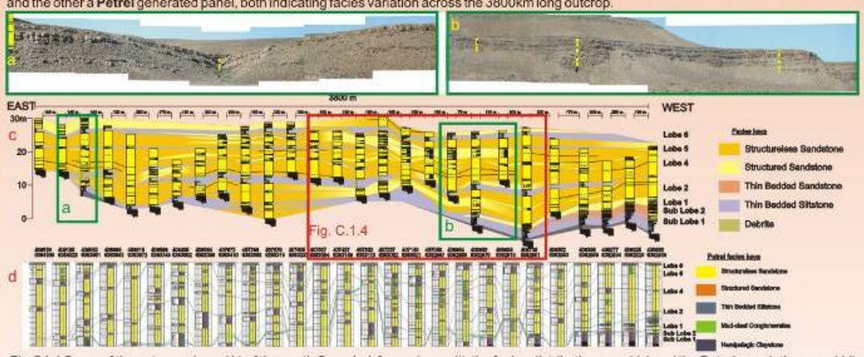

Fig.C1.1 Some of the outcrops (a and b) of the south Gemsbok face, along with the facies distribution panel (c) and the Petrel correlation panel (d).

3D Geological model

A **conceptual depositional model** was constructed using outcrop data and **isopachs** created in Petrel. The conceptual model was converted into a **grid** in Petrel and divided into 19 **zones** based on the **top and base surfaces** of lobes and lobe elements. The internal variation was simulated using **proportional layering**. Surface **topography** was left unchanged.

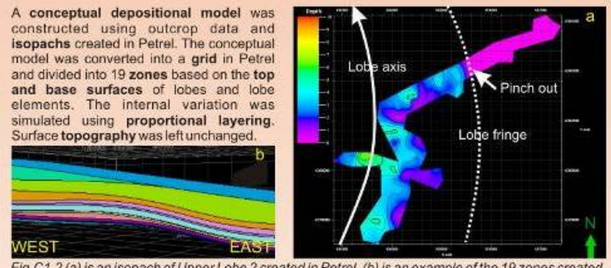

Fig.C1.2 (a) is an isopach of Upper Lobe 2 created in Petrel. (b) is an example of the 19 zones created. The zones represent 4 lobes, with 6 lobe elements (upper and lower lobes) and 9 interlobe units).

Reservoir model

The wells were upscaled into the 20mx20m **cells** of the grid, and the 3D distribution was simulated in 3D by using the **sequential Gaussian algorithm**.
The model is shown in Fig C1.3

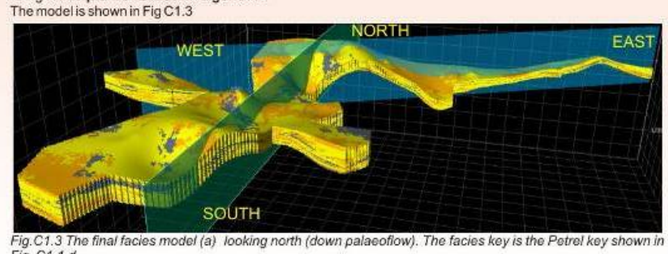

Fig.C1.3 The final facies model (a) looking north (down palaeoflow). The facies key is the Petrel key shown in Fig. C1.1.d.

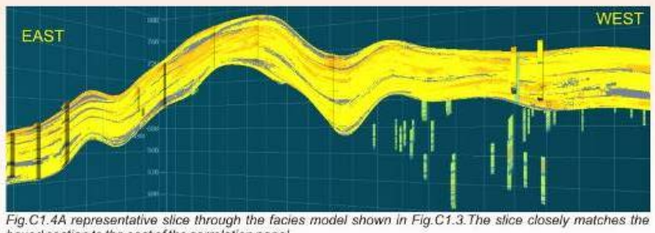

Fig.C1.4A representative slice through the facies model shown in Fig.C1.3.The slice closely matches the boxed section to the east of the correlation panel.

C2. Lobe axis to fringe (Middle Fan 2)

Outcrop observation

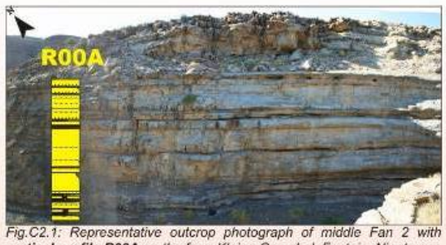

*Fig.C2.1: Representative outcrop photograph of middle Fan 2 with **vertical profile R00A** on the farm Kleine Gemsbok Fontein. Ninety-one vertical profiles were measured, representing Middle Fan 2 outcrop across the study area. Each profile depicts observations on sedimentary structures, facies and architectural elements.*

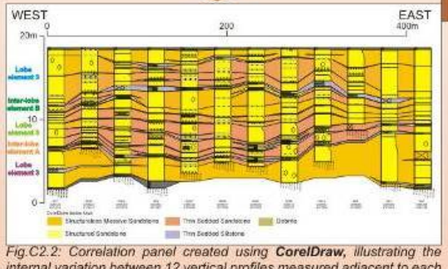

*Fig.C2.2: Correlation panel created using **CorelDraw,** illustrating the internal variation between 12 vertical profiles measured adjacent to each other on the farm Kleine Gemsbok Fontein. Middle Fan 2 is subdivided into three sandstone lobe elements separated by siltstone inter-lobe elements.*

3D geological model

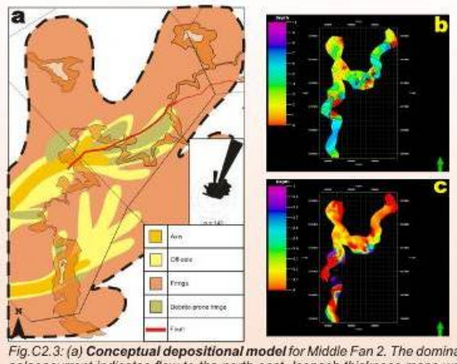

*Fig.C2.3: (a) **Conceptual depositional model** for Middle Fan 2. The dominant palaeocurrent indicates flow to the north-east. Isopach thickness maps were created for lobe element 1 (b) and inter-lobe element B (c), with hot colours indicating **thinner** elements .*

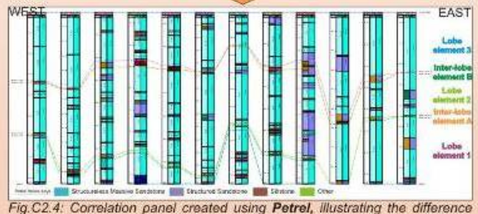

*Fig.C2.4: Correlation panel created using **Petrel,** illustrating the difference between input outcrop data (left) and output upscaled data (right). Input data represents 17 original facies, output data represents facies reduced to 5.*

Reservoir model

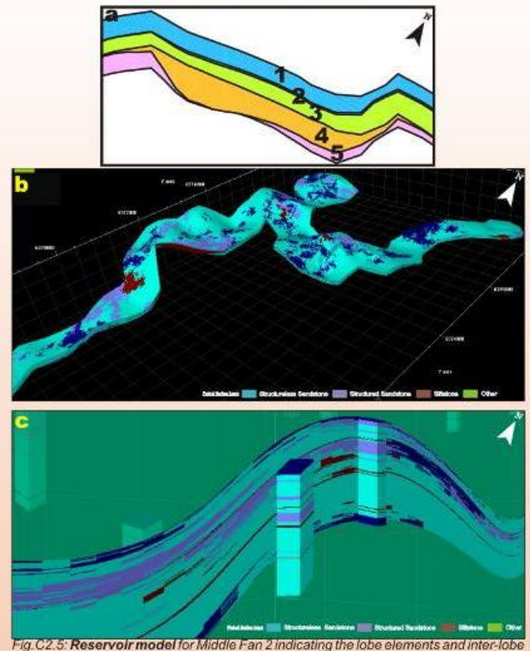

*Fig.C2.5: **Reservoir model** for Middle Fan 2 indicating the lobe elements and inter-lobe elements represented by 5 zones, each subdivided into layers (a), (b and c) the facies model for Middle Fan 2 and detail of the upscaled facies in the facies model.*

D. AUTOGENIC CONTROLS ON THE GEOMETRY AND STACKING PATTERN OF TERMINAL LOBE DEPOSITS

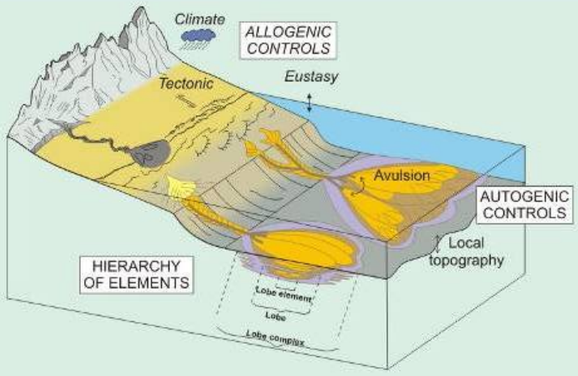

The architecture of submarine fans is governed by a multitude of processes, some of which may be classified as allogenic to a fan system, whereas others are considered autogenic.

Allogenic, or extrinsic, controls are those that force change in the architecture of the fan system *from the outside*. Examples of allogenic controls are mostly related to changes in the sediment supply signal (volume and frequency of flows, grain size of the source sediment), e.g., due to changes in relative sea level and climate, and changes in seafloor shelf-slope morphology due to tectonic activity.

Autogenic, or intrinsic, controls are those that cause changes in architecture due to processes occurring *in the fan system itself*. Autogenic behaviour in submarine fans is intimately related to the interplay between turbidity-current flow and sedimentation, which causes a subtle but complicated and dynamic depositional topography that strongly impacts the loci of erosion and deposition of subsequent flows and, therefore, the facies and thickness distributions of architectural elements.

D1. Finger like lobe geometry

Outcrop observation

Outcrops of Fan 3 demonstrate that planform geometries of lobes are not simple radial fan shapes . Commonly, lobes have finger-like projections near their termination, particularly basal lobes on a muddy substrate (see Section B3).

Interpretation

This cartoon map represents facies and thickness distributions within a typical Tanqua lobe. It attempts to **synthesise outcrop observations, isopach maps, and correlation panels.** There are no 'hard' lines between facies as these are transitional, and dotted lines represent axial pathways and indicate that there is not a single axis to a lobe. Smooth radial isopach contour lines are sketched here although in reality they are more complicated, particularly in areas close to pinchout.

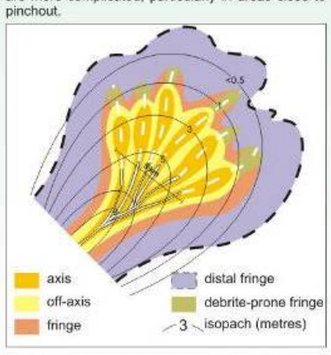

Fig D.1.1.:Cartoon map to represent facies and thickness distributions within a typical Tanqua lobe.

Process-based realisation

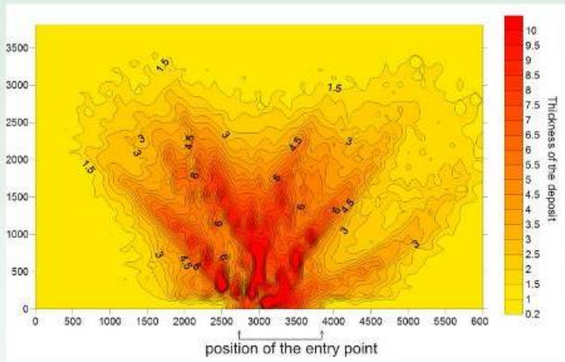

Aim:
To mimic the lateral shifts in the position of the mouth of a distributary channel due to avulsion, or a change in the axis of flow through a (depositional) shallow conduit. The position of the entry point of the flows into the model domain was varied on a flow-by-flow basis and in a disorganized manner.

Inflow position:
Inflow positions were randomly assigned from a distribution with a mean of 3000m and a standard deviation of 200 m. As such, all flows entered the domain of interest roughly between 2400 and 3600m.

Result:
Clearly, the disorganized shift in entry point results in an asymmetric stacking of beds which causes the depositional relief to be undulating, with elongated highs and lows in-between that widen downstream. Properties of this simulated lobe, such as the number of beds, overall thickness, volume and geometry, are in agreement with those observed at lobe scale in outcrop.

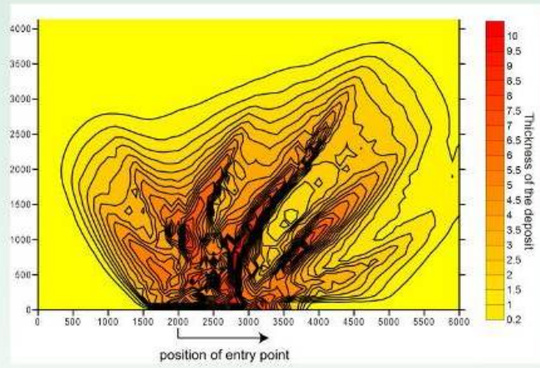

Aim:
To assess the influence of a more organized way of entry point switching, both in time and in space.

Inflow position:
The input parameters values are the same than in the previous example, but with flow entry points shifting from 2000 m to 3400 m and with steps of 100 m. Timing of the shifts was defined such that a shift occurred every three to four flows, depending on size and recurrence interval, which are randomly drawn from user-defined log normal distributions.

Result:
Elongate ridges now vary in length, and curve towards the right, i.e., in the direction of lateral shift of the entry point. Furthermore, flows seem to have preferentially followed one particular conduit, which therefore has resulted in bounding highs left and right that are more pronounced than the other highs, and also in transport of sediment further downstream. Evidently, the more organized shift of entry point, both in time and space, has resulted in a depositional relief with more pronounced highs with lows in-between that serve as pathways for several consecutive flows, which increases the distance over which sediment is transported.

D2. Compensational stacking patterns

Outcrop observation

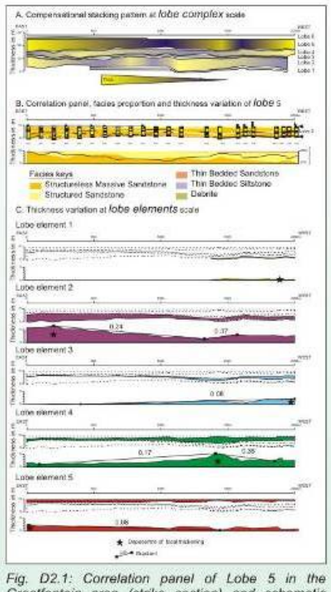

Fig. D2.1: Correlation panel of Lobe 5 in the Grootfontein area (strike section) and schematic correlation panels of individual lobe elements, highlighting distinct local thickening and thinning at lobe element scale, which is interpreted to result from the interaction of flows with depositional relief (compensational stacking).

Interpretation

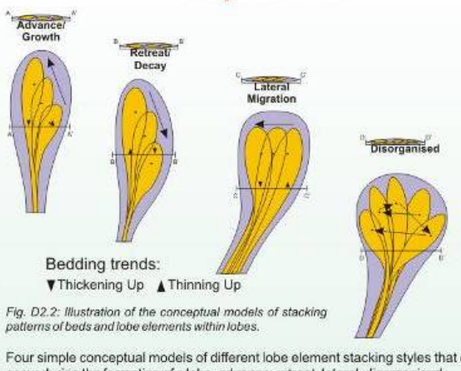

Fig. D2.2: Illustration of the conceptual models of stacking patterns of beds and lobe elements within lobes.

Four simple conceptual models of different lobe element stacking styles that can occur during the formation of a lobe, advance, retreat, lateral, disorganised.

Stacking Style 1: Advancement or Growth
This style could develop where the up-dip distributary channel is increasing in efficiency (channel lengthening) and/or sediment supply rate increases, although it could develop as an autogenic response to dynamic underlying topography.

Stacking Style 2: Retreat or Decay
This style could develop where the up-dip distributary channel is decreasing in efficiency (channel shortening) and/or sediment supply rate decreases, although it could develop as an autogenic response to dynamic underlying topography.

Stacking Style 3: Lateral Migration
This style could develop where sediment supply is quasi-stable, but the position of the distributary channel moves laterally (avulsion or open channel migration).

Stacking Style 4: Disorganised
This style could develop where the position of the up-dip distributary channel and/or the rate of sediment supply are unstable, although it could develop as an autogenic response to the developing underlying topography.

Process-based realisation

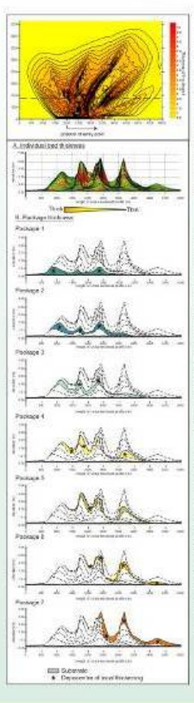

← *Fig. D2.3:* The cross-section is located at 900 m downstream of the entry point of the flows. The cross-section at the top displays the stratigraphy, with colour coding representing individual bed thickness. In the other cross-sections, individual beds have been grouped into 7 packages, based this time on the position of the entry point of the flows that deposited them, to highlight the effect of a systematic change in the position of a distributary channel-mouth or depositional conduit on the distribution of sediment and, consequently, organised stacking pattern at the scale of packages of beds. Each package is roughly equivalent in number of beds and volume to two lobe elements.

Fig. D2.4: →
The cross-section is located at 2200 m downstream of the entry point of the flows. The cross-section A displays the stratigraphy, with colour coding representing individual bed thickness. In the other cross-sections (B), individual beds have been grouped into four packages, based on spatial trends in bed thickness and grain size to illustrate lateral shifts in the locus of deposition due to the disorganized shift in entry points and the interaction of flows with depositional relief. Packages are equivalent in volume and number of beds to two to three outcrop-defined lobe elements. After Package 1, at any given time, deposition never occurs in a single area, i.e., it occurs simultaneously both to the left and right of Package 1, although at different rates.

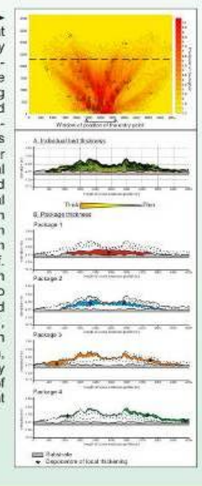

E. DISCUSSIONS AND CONLUSIONS

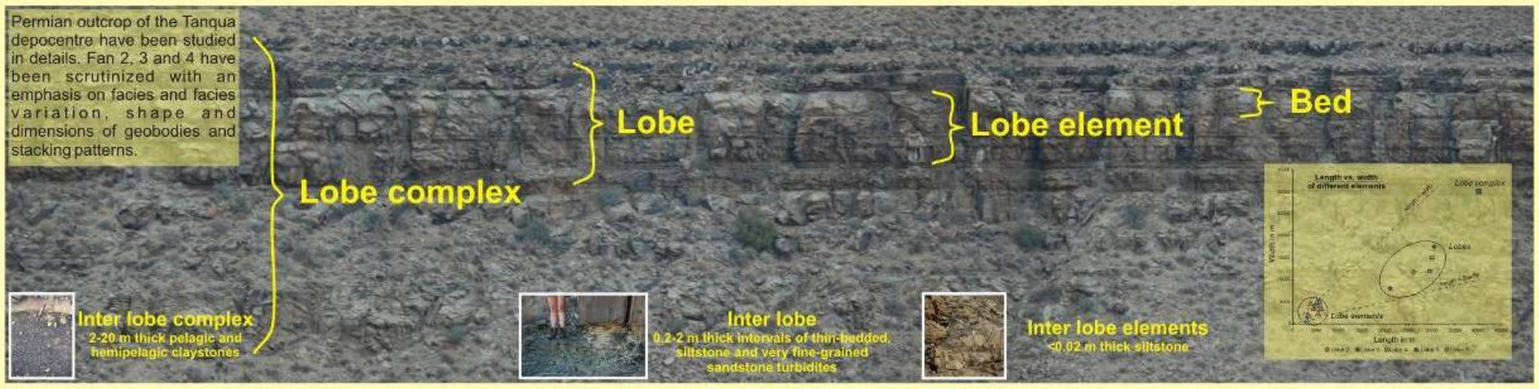

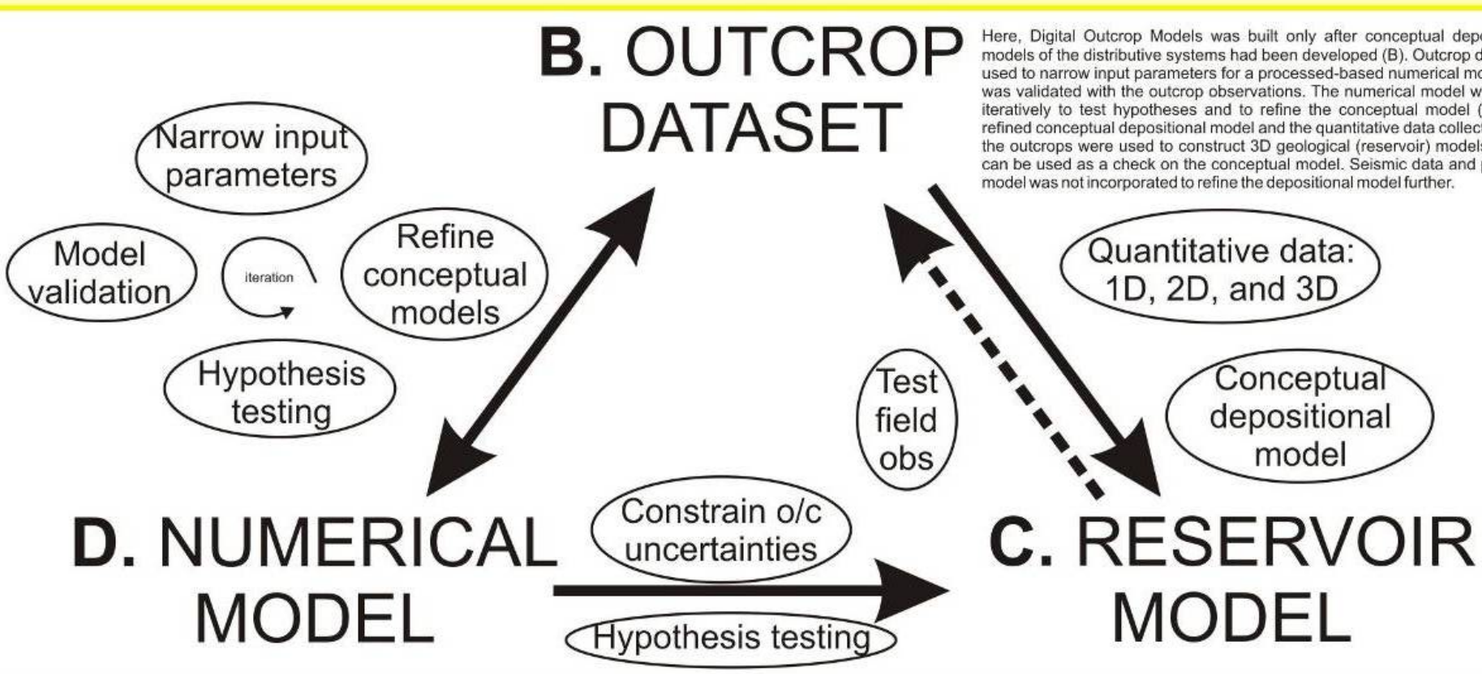

Here, Digital Outcrop Models was built only after conceptual depositional models of the distributive systems had been developed (B). Outcrop data was used to narrow input parameters for a processed-based numerical model that was validated with the outcrop observations. The numerical model was used iteratively to test hypotheses and to refine the conceptual model (D). The refined conceptual depositional model and the quantitative data collected from the outcrops were used to construct 3D geological (reservoir) models, which can be used as a check on the conceptual model. Seismic data and physical model was not incorporated to refine the depositional model further.

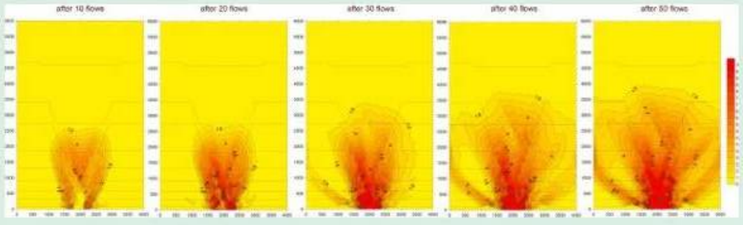

Outcrop studies give a good insight on turbidite reservoirs at interwells scale. However, the results obtained are mostly specific to the fan system under investigation, and extrapolation of findings to other fan systems often proves challenging. The 'process-based' approach focuses on the turbidity currents themselves. In addition, process-based numerical models provide a means to test and develop hypotheses developed from outcrop

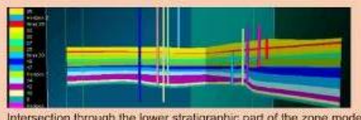

Intersection through the lower stratigraphic part of the zone model in the NB2 area. The left intersection is perpendicular to the Farm outcrop and crosses the Cliff outcrop. Vertical exaggeration is 20.

Example of lateral stacking driving by underlying depositional topography.

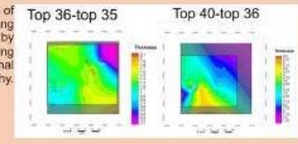

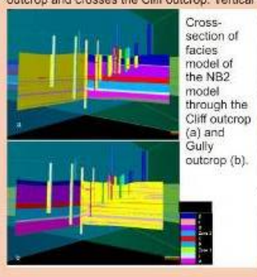

Cross-section of facies model of the NB2 model through the Cliff outcrop (a) and Gully outcrop (b).

The zone model for the NB2 area (built by Wieske Paulissen, TU Delft) represents several levels in the hierarchy of the lobe complex, and may provide insights into the trends of the zones and their stacking patterns. Since the NB2 model is based on a high-resolution field dataset it was possible to model a lobe element in one zone in the lower part of the stratigraphy and in one case even an individual bed (unit 36). Up stratigraphy, thicker packages were modelled in one zone which are lobes embedded in continuous siltstone- and mudstone-prone intervals.

E4. References

Fildani, A., Drinkwater, N.J., Weislogel, A., McHargue, T., Hodgson, D.M, Flint S.S. (2007) Age controls on the Tanqua and Laingsburg deep-water systems: New insights on the evolution and sedimentary fill of the Karoo basin, South Africa Source: Journal of sedimentary research, 77, 901 -908

Twichell DC, Schwab WC, Kenyon NH (1995) Geometry of sandy deposits at the distal edge of the Mississippi fan, Gulf of Mexico. In: Pickering KT, Hiscott RN, Kenyon NH, Ricci Lucchi F, Smith RDA (eds) Atlas of deep water environments: architectural style in turbidite systems. Chapman and Hall, London, pp 282–286

Wickens H de V (1994) Basin floor fan building turbidites of the southwestern Karoo Basin, Permian Ecca Group, South Africa. PhD Thesis, Univ Port Elisabeth, 233 pp

E5. Acknowledgments

The authors wish to thanks the LOBE consortium: Chevron, Maersk Oil, Petrobras, Petro SA, Shell, StatoilHydro and Total for sponsorising several studenships. Most of the reservoir modelling with Petrel® licences provided by Schlumberger, and the work was completed at PetroSA Cape Town and we are especially grateful for the help we received from Jody Frewin. Laura McAllister, Emily Parrott and John Kavanagh are thanks for field assistance.